

# Nonlinear response theory for lossy superconducting quantum circuits

V. Vadimov,<sup>1,\*</sup> M. Xu,<sup>2</sup> J. T. Stockburger,<sup>2</sup> J. Ankerhold,<sup>2</sup> and M. Möttönen<sup>1,3</sup>

<sup>1</sup>*QCD Labs, QTF Centre of Excellence, Department of Applied Physics, Aalto University, P.O. Box 15100, FI-00076 Aalto, Finland*

<sup>2</sup>*Institute for Complex Quantum Systems and IQST, Ulm University - Albert-Einstein-Allee 11, D-89069 Ulm, Germany*

<sup>3</sup>*VTT Technical Research Centre of Finland Ltd, QTF Centre of Excellence, P.O. Box 1000, FI-02044 VTT, Finland*

(Dated: October 25, 2023)

We introduce a numerically exact and yet computationally feasible nonlinear response theory developed for lossy superconducting quantum circuits based on a framework of quantum dissipation in a minimally extended state space. Starting from the Feynman-Vernon path integral formalism for open quantum systems with the system degrees of freedom being the nonlinear elements of the circuit, we eliminate the temporally non-local influence functional of all linear elements by introducing auxiliary harmonic modes with complex-valued frequencies coupled to the non-linear degrees of freedom of the circuit. In our work, we propose a concept of time-averaged observables, inspired by experiment, and provide an explicit formula for producing their quasiprobability distribution. Furthermore, we systematically derive a weak-coupling approximation in the presence of a drive, and demonstrate the applicability of our formalism through a study on the dispersive readout of a superconducting qubit. The developed framework enables a comprehensive fully quantum-mechanical treatment of nonlinear quantum circuits coupled to their environment, without the limitations of typical approaches to weak dissipation, high temperature, and weak drive. Furthermore, we discuss the implications of our findings to the quantum measurement theory.

## I. INTRODUCTION

Quantum systems inherently interact with their environments, typically consisting of a macroscopic number of degrees of freedom [1–3]. These interactions give rise to a diverse range of phenomena, including decoherence, dissipation-induced phase transitions [4, 5], and emergence of classical physics in quantum systems [6] among many others [3]. Understanding and accurately describing the dynamics of open quantum systems is of fundamental importance in various fields, ranging from quantum information science and quantum computing [7–10] to condensed matter physics [11] and quantum optics [1, 12]. Recent technological advances [13–20] have opened up new possibilities for experimental studies of open quantum systems, necessitating the development of accurate and computationally efficient theoretical models.

Traditional Markovian approaches [1, 21–23] for treating open quantum systems rely on assumptions of weak coupling and time-scale separation of the system and the bath, or substantially high temperature, which may not always hold in experimentally relevant setups leading to non-Markovian dynamics [24–30]. Furthermore, these approaches may have limited applicability in the presence of structured reservoirs with gaps or other singularities in the spectral density. Non-perturbative treatments often involve discretization of the bath [31, 32] or employ the Feynman-Vernon path integral formalism [33]. The latter includes techniques such as path integral Monte Carlo

(PIMC) [34–37], unraveling the time-nonlocal influence functional using auxiliary stochastic fields [38, 39], introducing a set of auxiliary density operators governed by a system of time-local hierarchical equations of motion (HEOM) [40, 41], and others [42–46]. Recently, a broad variety of numerically exact methods has been unified within the framework of quantum dissipation in a minimally extended state space (QD-MESS) [47, 48] which provides high accuracy with relatively moderate computational resources.

In addition to the inevitable interaction with the natural environment, the study of open quantum systems is also motivated by the need to carry out measurements on real quantum systems [49]. In such cases, the measurement apparatus itself acts as an environment, leading to controllable decoherence. In this setup standard von Neumann measurements [50] can be performed only on the macroscopic measurement device or its part [49], hence a single measurement gives a very limited information about the system of interest. This has two consequences: first, no real measurement is instantaneous since the result usually comes from integration of continuous measurements, and second, even continuous measurements performed with a specific device cannot provide access to arbitrary observables of the system of interest.

In many experimental setups it is common to probe the electromagnetic field [51] emitted from the measured system. To this end, the input-output (IO) theory [52–54] for quantum optical systems and superconducting quantum circuits was developed to calculate the properties of the emitted far-field radiation and its integral characteristics. A major advantage of the IO theory is the possi-

---

\* vasilii.l.vadimov@aalto.fi

bility to generalize it for quantum networks [55], where the output from one part of the system may serve as the input for another part. These theories are quite accurate in quantum optical systems but rely on the Born–Markov approximation, which may break down, e.g., in the strong coupling regime. In fact, non-Markovian effects may be more pronounced in microwave superconducting circuits [29, 30] which are among the leading platforms for quantum computing applications [51, 56, 57]. Effects of retardation and correlations between the system and environment are critical for the design and optimization of superconducting qubits, quantum gates, initialization, and readout protocols, especially in circuits with tunable dissipative elements [16, 58–61] and distributed-element qubits [62]. Thus, a rigorous and computationally efficient IO theory that goes beyond the limitations of Markov approximations is essential for accurate characterizing and harnessing the dynamics of superconducting circuits.

The first non-Markovian IO theory was presented in Ref. [63] based on temporally non-local Heisenberg equations of motion for the degrees of freedom of the system and the field operators in the case of a one-dimensional chiral field propagating in one direction. However, solving these equations can be technically involved for nonlinear systems. Later, this approach was generalized for quantum networks [64] and squeezed input fields [65]. In other studies [66, 67], the IO formalism was developed for atoms in a cavity which is coupled to a Markovian bath.

Due to the approximation of the chiral field, it is infeasible to properly account for thermal effects. This approximation introduces negative-frequency modes, which do not have a thermal state at a positive temperature. It is a reasonable approximation in quantum optics, since the characteristic frequency scale is much higher than the temperature scale, especially if the back-scattering can be neglected. This is not the case for the superconducting quantum circuits, where thermal effects are important and reflections from the qubits and resonators are usually strong.

The main goal of this paper is to develop a general formalism for dissipative superconducting quantum circuits which goes beyond the Born–Markov approximation, utilizing modern techniques for open quantum systems. We refer to this formalism as nonlinear response (NLR) theory. In superconducting circuits, the sources and measurement devices of the microwave field are typically connected to other components by dispersion-free coaxial or coplanar waveguides. These transmission lines act as dissipation channels, in addition to dielectric losses [68, 69] or quasiparticles in the superconductors [70–74].

In our formalism, we utilize the QD-MESS approach and account for the non-Markovian environment which is represented by finite number of damped bosonic modes [47, 75] coupled to the nonlinear degrees of freedom of the circuit. By incorporating these auxiliary modes, we can capture the full non-Markovian dynam-

ics induced by the system-environment interaction, including memory effects and correlations. Our formalism provides a systematic framework for studying the input-output characteristics of the circuit, taking into account the interplay between the dissipation, the nonlinearity of the circuit, and the external driving fields. The suggested approach is similar to the black-box quantization technique [76, 77], however it is free from the limitation of weak dissipation [76] and the need of bath discretization [77].

The structure of the paper is as follows: In Sec. II, we provide a brief introduction to the Caldeira–Leggett model, which describes a broad class of dissipative quantum systems, and establish the connections between classical Langevin equations and the influence functional components in Keldysh space. We focus the remainder of the paper on the study of superconducting quantum circuits. Section III contains the central result of our paper, presenting a detailed derivation of the NLR theory. Starting from the classical Kirchhoff’s law for the circuit and the insights gained from Sec. II, we derive the action on the Keldysh contour for the circuit. We explicitly incorporate classical driving and introduce a quantum source or counting field to obtain the generating functional of the output field. We then proceed to eliminate the linear degrees of freedom of the circuit and unravel the resulting time-nonlocal influence functional by introducing auxiliary bosonic modes. This leads to a time-local QD-MESS equation that governs the dynamics of the open quantum system. We define observables as time averages of the output field and provide an explicit formula for their quasiprobability distribution through the generating functional. In Sec. IV, we focus on the systematic derivation of the weak-coupling regime in the presence of possibly strong driving fields, which are non-trivial to accommodate exactly in master equations. The coupling to off-resonant auxiliary modes can be eliminated through the use of a dynamical Schrieffer–Wolf transformation [78, 79]. In Sec. V, we illustrate our theory by applying it to the problem of dispersive readout of a superconducting transmon qubit. Finally, we summarize our findings and provide our conclusions in Sec. VI.

## II. CALDEIRA–LEGGETT MODEL

Throughout the paper we use the following notation: Lowercase bold characters denote vectors, uppercase bold characters denote matrices. A bold capital character with subscripts denotes a certain block of the matrix denoted by the corresponding character. Functions of time and frequency denoted by the same character are related to

each other by Fourier transformation:

$$X(\omega) = \int_{-\infty}^{+\infty} X(t)e^{i\omega t} dt, \quad (1)$$

$$X(t) = \frac{1}{2\pi} \int_{-\infty}^{+\infty} X(\omega)e^{-i\omega t} dt. \quad (2)$$

The operators in the Hilbert space are emphasized by  $\hat{\cdot}$  accent, the operators in the extended Liouville space are denoted by  $\check{\cdot}$  accents.

We begin our analysis by considering the paradigmatic Caldeira–Leggett model [80] for dissipative systems. The classical Lagrangian of this model is given by

$$\begin{aligned} \mathcal{L}(\dot{x}, \dot{q}_k, x, q_k, t) &= \frac{m\dot{x}^2}{2} - V(x, t) \\ &+ \sum_k \left[ \frac{m_k \dot{q}_k^2}{2} - \frac{m_k \omega_k^2}{2} \left( q_k - \frac{c_k}{m_k \omega_k^2} x \right)^2 \right], \end{aligned} \quad (3)$$

which describes a particle of mass  $m$  in a possibly time-dependent potential  $V(x, t)$  interacting with a plethora of environmental harmonic oscillators each with mass  $m_k$ , bare angular frequency  $\omega_k$ , and coupling constant  $c_k$  which provides the coupling between the system and the  $k$ :th oscillator. The Feynman–Vernon path integral approach [33] is the conventional quantum-mechanical treatment of this system. The time evolution of the full density matrix of the system  $W(\mathbf{x}_+, \mathbf{x}_-, t)$  from time  $t^i$  to  $t^f > t^i$  can be found as

$$\begin{aligned} W(\mathbf{x}_+^f, \mathbf{x}_-^f, t^f) &= \int K(\mathbf{x}_+^f, \mathbf{x}_-^f, t^f; \mathbf{x}_+^i, \mathbf{x}_-^i, t^i) \\ &W(\mathbf{x}_+^i, \mathbf{x}_-^i, t^i) d\mathbf{x}_+^i d\mathbf{x}_-^i, \end{aligned} \quad (4)$$

where the subscripts “+” and “−” stand for the first and the second arguments of the density matrix, respectively,  $\mathbf{x}_\pm = [x_\pm \ q_{1,\pm} \ q_{2,\pm} \ \dots]^T$  are vectors of all coordinates of all the degrees of freedom, and the propagator  $K(\dots)$  is given by the following path integral:

$$K(\dots) = \int \mathcal{D}[\mathbf{x}_+, \mathbf{x}_-] \exp \left\{ \frac{i}{\hbar} (S[\mathbf{x}_+] - S[\mathbf{x}_-]) \right\}. \quad (5)$$

Here, the path integration is carried out over the fixed-boundary trajectories  $\mathbf{x}_\pm(t^{i/f}) = \mathbf{x}_\pm^{i/f}$  and the functional  $S[\mathbf{x}]$  is a classical action

$$S[\mathbf{x}] = \int_{t^i}^{t^f} \mathcal{L}(\dot{\mathbf{x}}, \mathbf{x}, t) dt. \quad (6)$$

It is convenient to carry out a Keldysh rotation to so-called classical and quantum trajectories [11]

$$\mathbf{x}_\pm = \mathbf{x}_c \pm \frac{\mathbf{x}_q}{2}. \quad (7)$$

The choice of the Keldysh formulation for the path integral is justified by its simplicity in the coupling to the external fields: classical fields couple to quantum degrees of freedom of the system, and quantum counting fields couple to classical degrees of freedom. We utilize this substitution in the path integral (5), consider the limit  $t^i \rightarrow -\infty$  and  $t^f \rightarrow +\infty$ , and assume that the full system was initially in a thermal state at temperature  $T$ . The drive, if there is any, is assumed to be off in the past  $\check{V}(x, t) \rightarrow 0$  at  $t \rightarrow -\infty$ . We calculate the trace over all degrees of freedom and obtain unity

$$1 = \int \mathcal{D}[\mathbf{x}_c, \mathbf{x}_q] \exp \left\{ \frac{i}{\hbar} S[\mathbf{x}_c, \mathbf{x}_q] \right\}, \quad (8)$$

where the Keldysh action is given by [11]

$$\begin{aligned} S[\mathbf{x}_c, \mathbf{x}_q] &= \int_{-\infty}^{+\infty} \left\{ \frac{m}{2} [x_c \ x_q] \mathbf{D}^{-1}(i\partial_t) \begin{bmatrix} x_c \\ x_q \end{bmatrix} \right. \\ &- V\left(x_c + \frac{x_q}{2}, t\right) + V\left(x_c - \frac{x_q}{2}, t\right) \\ &+ \sum_k \left[ \frac{m_k}{2} [q_{k,c} \ q_{k,q}] \mathbf{D}^{-1}(i\partial_t) \begin{bmatrix} q_{k,c} \\ q_{k,q} \end{bmatrix} \right. \\ &\left. \left. - \omega_k^2 \left( q_{k,c} - \frac{c_k x_c}{m_k \omega_k^2} \right) \left( q_{k,q} - \frac{c_k x_q}{m_k \omega_k^2} \right) \right] \right\}. \end{aligned} \quad (9)$$

Here, we introduced an inverse Green’s function

$$\mathbf{D}^{-1}(\omega) = \begin{bmatrix} 0 & (\omega - i0^+)^2 \\ (\omega + i0^+)^2 & 2i0^+ \omega \coth\left(\frac{\hbar\omega}{2k_B T}\right) \end{bmatrix}, \quad (10)$$

where  $\mathbf{D}^{-1}(i\partial_t)$  stands for the function of the differential operator. The symbol  $0^+$  should be treated as an infinitesimal positive frequency introduced to provide proper causality. The quantum-classical and classical-quantum components are the retarded and advanced inverse Green’s functions of a free classical particle with unit mass, respectively. The quantum-quantum or Keldysh component is a time non-local regularization which arises from the thermal initial condition in the action.

The action is quadratic in the bath degrees of freedom, and hence the path integral over them can be evaluated explicitly. We obtain an effective action for the system coordinate as

$$\begin{aligned} S_s[x_c, x_q] &= -i\hbar \ln \left( \int \mathcal{D}[q_{k,c}, q_{k,q}] \exp \left\{ \frac{i}{\hbar} S[\mathbf{x}_c, \mathbf{x}_q] \right\} \right). \end{aligned} \quad (11)$$

This effective action is given by

$$S_s[x_c, x_q] = \int_{-\infty}^{+\infty} \left[ m\dot{x}_c\dot{x}_q - V\left(x_c + \frac{x_q}{2}, t\right) + V\left(x_c - \frac{x_q}{2}, t\right) \right] dt - \frac{1}{2} \int_{-\infty}^{+\infty} [x_c(t) \ x_q(t)] \Sigma(t-t') \begin{bmatrix} x_c(t') \\ x_q(t') \end{bmatrix} dt dt', \quad (12)$$

where the integration over bath degrees of freedom results in the emergence of a finite time non-local term called influence functional [33]. We refer to the kernel of this functional  $\Sigma(t-t')$  as self-energy in analogy with the self-energy from condensed matter physics. The self-energy has a similar structure to that of the inverse Green's function, namely,

$$\Sigma(\omega) = \begin{bmatrix} 0 & \Sigma^A(\omega) \\ \Sigma^R(\omega) & \Sigma^K(\omega) \end{bmatrix} \quad (13)$$

and  $\Sigma(t-t')$  is its Fourier image

$$\Sigma(t-t') = \frac{1}{2\pi} \int_{-\infty}^{+\infty} \Sigma(\omega) e^{-i\omega(t-t')} d\omega. \quad (14)$$

The retarded component  $\Sigma^R(\omega)$  is a classical force-coordinate response function of the bath, the advanced component, extended to the whole complex frequency plane,  $\Sigma^A(\omega) = [\Sigma^R(\omega^*)]^*$  is its conjugate, and the Keldysh component is given by the fluctuation dissipation theorem as

$$\Sigma^K(\omega) = \frac{1}{2} [\Sigma^R(\omega) - \Sigma^A(\omega)] \coth\left(\frac{\hbar\omega}{2k_B T}\right). \quad (15)$$

By applying the Hubbard–Stratonovich transformation to the Keldysh part of the influence functional (12) and employing a saddle-point approximation, we obtain the quasiclassical Langevin equation for the system as [11, 81]

$$-m\ddot{x}_c - \int_{-\infty}^{+\infty} \Sigma^R(t-t')x_c(t') dt' - \frac{\partial V(x_c, t)}{\partial x_c} = \xi(t), \quad (16)$$

where  $\xi(t)$  is a Gaussian-noise term with the correlation function

$$\langle \xi(t)\xi(t') \rangle = \frac{i}{2\pi} \int_{-\infty}^{+\infty} \Sigma^K(\omega) e^{-i\omega(t-t')} d\omega. \quad (17)$$

A quantum counterpart of this equation is a Heisenberg–Langevin equation [82–84] which is written for coordinate operators and has an operator-valued noise term with Gaussian statistics. However, its direct application

beyond linear systems is complicated due to the lack of a closed system of equations for correlation functions.

The main conclusion from this section is that in order to construct the Feynman–Vernon influence functional, it is enough to know only the classical response function of the bath and its temperature. If we do not have a microscopic model for the bath, but know its classical response function, we can introduce the corresponding terms phenomenologically into the Keldysh action.

### III. NONLINEAR RESPONSE THEORY FOR QUANTUM CIRCUITS

Although many parts of this theory are general and agnostic to the physical realization, we motivate our studies by a particular class of open quantum systems, namely, superconducting quantum circuits. We consider circuits formed by lumped elements with linear elements such as capacitors, inductors, Ohmic resistors, and nonlinear elements such as Josephson junctions. Due to their inherent nonlinearity, the latter are the key components of every superconducting qubit. The control and the measurement of the circuit is provided by coupling to semi-infinite transmission lines, which inevitably introduce additional dissipation channels in the system.

Such systems indeed fall into the Caldeira–Legett class of systems. However, from the experimental point of view, not all of its observables can be probed directly. The only experimentally accessible quantities are the output fields in the transmission lines, which belong rather to the environment. As we further discuss below, the whole division between the system and the environment may be ambiguous. Therefore, there is a need of a theory which connects the classical drive field with the experimentally observable output field.

#### A. Classical equations of motion

Using conclusions from the previous section, we begin with writing classical equations of motion for the electric circuit [85]. We define the flux  $\varphi_k$  for each node  $k$  of the circuit and express Kirchhoff's law for it as

$$-\sum_{k'} C_{kk'} (\dot{\varphi}_k - \dot{\varphi}_{k'}) - \sum_{k'} \frac{\dot{\varphi}_k - \dot{\varphi}_{k'}}{R_{kk'}} - \sum_{k'} \frac{\varphi_k - \varphi_{k'}}{L_{kk'}} - \sum_{k'} i_{J,kk'} - \sum_j \frac{\dot{\varphi}_k - 2v_{i,(kj)}}{Z_{(kj)}} = 0, \quad (18)$$

where the first four sums describe the currents coming into the node  $k$  from capacitors  $C_{kk'}$ , resistors  $R_{kk'}$ , inductors  $L_{kk'}$ , and Josephson junctions which connect it to the other nodes  $k'$ , whereas the last sum corresponds to the current coming from the transmission lines with characteristic impedances  $Z_{(kj)}$  coupled to the node  $k$  as

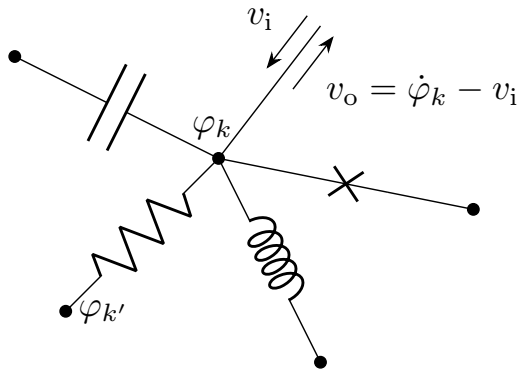


FIG. 1. Node  $k$  with flux  $\varphi_k$ , connected to a transmission line and other nodes via capacitors, resistors, inductors, and Josephson junctions. The output voltage in the transmission line is determined by the input voltage and the voltage given by  $\dot{\varphi}_k$ .

illustrated in Fig. 1. Here, index  $j$  in a pair  $(kj)$  enumerates all the transmission lines connected to the node  $k$ . The Josephson current is given by

$$i_{J,kk'} = \frac{2\pi E_{J,kk'}}{\Phi_0} \sin \left[ \frac{2\pi}{\Phi_0} (\varphi_k - \varphi_{k'} - \Phi_{kk'}) \right], \quad (19)$$

where  $E_{J,kk'}$  is the Josephson energy of the junction between the nodes  $k$  and  $k'$ ,  $\Phi_{kk'}$  is the flux bias of the junction, and  $\Phi_0$  is the superconducting flux quantum. If a pair of nodes  $k$  and  $k'$  is not connected by a capacitor then we put  $C_{kk'} = 0$ . For the same cases related to resistors, inductors, and Josephson junctions we put  $R_{kk'} \rightarrow \infty$ ,  $L_{kk'} \rightarrow \infty$ , and  $E_{J,kk'} = 0$ . If there is a ground node in the circuit, we put the corresponding flux  $\varphi_{\text{ground}} = 0$ . The output  $v_{o,(kj)}$  voltage in the transmission line  $j$  connected to the node  $k$  can be expressed through the input field and the voltage at the node as

$$v_{o,(kj)} = \dot{\varphi}_k - v_{i,(kj)} \quad (20)$$

since the voltage at the node  $v_{o,(kj)} + v_{i,(kj)} = \dot{\varphi}_k$  must be single-valued for all transmission lines  $j$  connected to the node  $k$ .

We rewrite Eq. (18) in the matrix form, introducing notations  $\boldsymbol{\varphi}$  as vector of the fluxes at all the nodes,  $\mathbf{v}_{i/o}$  as vectors of input and output voltages in the transmission lines, and  $\mathbf{i}_J$  as vector of currents through all the Josephson junctions:

$$\mathbf{K}^{\text{R}}(i\partial_t) \begin{bmatrix} \boldsymbol{\varphi} \\ \mathbf{v}_i \end{bmatrix} = \begin{bmatrix} \nabla^{\text{T}} \mathbf{i}_J \\ \mathbf{v}_o \end{bmatrix}, \quad (21)$$

where the frequency dependent matrix  $\mathbf{K}^{\text{R}}(\omega)$  describes the causal response of the linear elements, and matrix  $\nabla^{\text{T}}$  is a discrete divergence matrix for the Josephson currents. The explicit expression for the elements of the matrix  $\mathbf{K}^{\text{R}}(\omega)$  can be obtained by applying a Fourier transformation to Kirchhoff's law and the input-output relations. The matrix  $\mathbf{K}^{\text{R}}(\omega)$  has a block structure, where blocks

correspond to the linear coupling between dynamical degrees of freedom and input and output fields:

$$\mathbf{K}^{\text{R}}(\omega) = \begin{bmatrix} \mathbf{K}_{\varphi\varphi}^{\text{R}}(\omega) & \mathbf{K}_{\varphi i}^{\text{R}}(\omega) \\ \mathbf{K}_{o\varphi}^{\text{R}}(\omega) & \mathbf{K}_{oi}^{\text{R}}(\omega) \end{bmatrix}. \quad (22)$$

The first block  $\mathbf{K}_{\varphi\varphi}^{\text{R}}(\omega)$  describes the linear coupling between the nodes:

$$K_{\varphi\varphi;kk'}^{\text{R}}(\omega) = \sum_j \frac{i\omega}{Z_{(kj)}} \delta_{kk'} - (-1)^{\delta_{kk'}} \left( \omega^2 C_{kk'} + \frac{i\omega}{R_{kk'}} - \frac{1}{L_{kk'}} \right). \quad (23)$$

The block  $\mathbf{K}_{\varphi i}^{\text{R}}(\omega)$  describes the coupling to the driving field:

$$K_{\varphi\varphi;k(k'j)}^{\text{R}} = \frac{2}{Z_{kj}} \delta_{kk'}. \quad (24)$$

The latter blocks provide the expression of the output field through the node fluxes and input voltages:

$$\begin{aligned} K_{o\varphi;(kj)k'}^{\text{R}}(\omega) &= -i\omega \delta_{kk'}, \\ K_{oi;(kj)(k'j')}^{\text{R}}(\omega) &= -\delta_{kk'} \delta_{jj'}. \end{aligned} \quad (25)$$

Note that the matrix  $\mathbf{K}^{\text{R}}(\omega)$  is nothing but the retarded component of the self-energy coming from the dissipation channels, combined with the contributions from the linear reactive elements.

## B. Keldysh action

Let us write down the Keldysh action for the considered circuit, assuming that all the dissipation channels are described by a uniform temperature  $T$ . The full information on the dynamics of the circuit and its observables is stored in the corresponding generating functional [11]. This can be expressed through a path integral

$$\mathcal{Z}[\mathbf{v}_i, \boldsymbol{\eta}_o] = \int \mathcal{D}[\boldsymbol{\varphi}_c, \boldsymbol{\varphi}_q] \exp \left\{ \frac{i}{\hbar} S_{\text{circ}}[\boldsymbol{\phi}] \right\}, \quad (26)$$

where  $\boldsymbol{\phi} = [\boldsymbol{\varphi}_c^{\text{T}} \ \mathbf{v}_i^{\text{T}} \ \boldsymbol{\varphi}_q^{\text{T}} \ \boldsymbol{\eta}_o^{\text{T}}]^{\text{T}}$ ,  $\boldsymbol{\varphi}_c$  and  $\boldsymbol{\varphi}_q$  stand for classical and quantum trajectories of the dynamical degrees of freedom  $\boldsymbol{\varphi}$ , and  $\boldsymbol{\eta}_o$  is an auxiliary quantum field which is an argument of the generating functional. The latter plays the role of a counting field used to generate the statistics of observables [2, 11] The action of the circuit  $S_{\text{circ}}[\boldsymbol{\phi}]$  is given by

$$S_{\text{circ}}[\boldsymbol{\phi}] = S_J[\boldsymbol{\varphi}_c, \boldsymbol{\varphi}_q] + \frac{1}{4\pi} \int_{-\infty}^{+\infty} \boldsymbol{\phi}^{\dagger}(\omega) \mathbf{G}^{-1}(\omega) \boldsymbol{\phi}(\omega) d\omega, \quad (27)$$

where

$$S_J[\varphi_c, \varphi_q] = - \int_{-\infty}^{+\infty} V_J[\varphi_c(t), \varphi_q(t)] dt \quad (28)$$

and

$$V_J(\varphi_c, \varphi_q) = 2 \sum_{k < k'} E_{J, k k'} \sin \left[ \frac{2\pi (\psi_{c, k k'} - \Phi_{k k'})}{\Phi_0} \right] \sin \left( \frac{\pi \psi_{q, k k'}}{\Phi_0} \right). \quad (29)$$

is the action for Josephson junctions and  $\psi_{c/q, k k'} = \varphi_{c/q, k} - \varphi_{c/q, k'}$  are the classical and quantum variables for the flux difference across the junction between the nodes  $k$  and  $k'$ . The inverse bare Green's function assumes the form

$$\mathbf{G}^{-1}(\omega) = \begin{bmatrix} \mathbf{0} & \mathbf{K}^A(\omega) \\ \mathbf{K}^R(\omega) & \mathbf{K}^K(\omega) \end{bmatrix}. \quad (30)$$

The retarded component is the same matrix  $\mathbf{K}^R(\omega)$  introduced in the previous subsection, the advanced component is its hermitian conjugate

$$\mathbf{K}^A(\omega) = [\mathbf{K}^R(\omega^*)]^\dagger, \quad (31)$$

and the Keldysh component is determined by the fluctuation dissipation theorem

$$\mathbf{K}^K(\omega) = \frac{1}{2} \coth \left( \frac{\hbar\omega}{2k_B T} \right) \begin{bmatrix} \mathbf{K}_{\varphi\varphi}^R(\omega) - \mathbf{K}_{\varphi\varphi}^A(\omega) & 0 \\ 0 & 0 \end{bmatrix}. \quad (32)$$

In addition to the classical driving field  $\mathbf{v}_i$ , we have introduced an auxiliary quantum source  $\boldsymbol{\eta}_o$  which couples to the output field in the transmission lines. The saddle-point approximation with respect to the quantum degrees of freedom and the quantum source  $\boldsymbol{\eta}_o$  yields the classical equations of motion (21).

It is convenient to use vectors  $\boldsymbol{\psi}_{c/q}$  of all classical and quantum flux differences across all junctions as dynamical variables. By doing so, we move from a node description of the electric circuit to an element description. For simplicity, we assume that there are no Josephson junction loops since otherwise we need to pick a minimal set of linearly independent variables which fully parametrize the Josephson energy of the circuit. They should be complemented by dynamical variables  $\boldsymbol{\psi}'_{c/q}$  such that a linear transformation of chosen real-valued matrices  $\mathbf{Q}_{\varphi\psi}$  and  $\mathbf{Q}_{\varphi\psi'}$

$$\boldsymbol{\varphi}_{c/q} = [\mathbf{Q}_{\varphi\psi} \quad \mathbf{Q}_{\varphi\psi'}] \begin{bmatrix} \boldsymbol{\psi}_{c/q} \\ \boldsymbol{\psi}'_{c/q} \end{bmatrix} \quad (33)$$

is reversible. Note that the action becomes quadratic with respect to the  $\boldsymbol{\psi}'$  degrees of freedom, and hence they can be integrated out. By doing this, we shift the

boundary between the system and environment and consider the linear subcircuit as part of the environment. The subcircuit of remaining nonlinear elements we refer to as core system. The effective action arising from the Gaussian integration over these degrees of freedom is given by

$$S_{\text{core}}[\boldsymbol{\phi}_{\text{core}}] = S_J[\boldsymbol{\psi}_c, \boldsymbol{\psi}_q] - \frac{1}{4\pi} \int_{-\infty}^{+\infty} \boldsymbol{\phi}_{\text{core}}^\dagger(\omega) \boldsymbol{\Sigma}_{\text{core}}(\omega) \boldsymbol{\phi}_{\text{core}}(\omega), \quad (34)$$

where  $\boldsymbol{\phi}_{\text{core}} = [\boldsymbol{\psi}_c^\top \quad \mathbf{v}_i^\top \quad \boldsymbol{\psi}_q^\top \quad \boldsymbol{\eta}_o^\top]^\top$  and the self-energy becomes

$$\boldsymbol{\Sigma}_{\text{core}}(\omega) = \begin{bmatrix} \mathbf{0} & \boldsymbol{\Sigma}_{\text{core}}^A(\omega) \\ \boldsymbol{\Sigma}_{\text{core}}^R(\omega) & \boldsymbol{\Sigma}_{\text{core}}^K(\omega) \end{bmatrix} = \tilde{\mathbf{G}}_{\boldsymbol{\phi}\boldsymbol{\psi}'}^{-1}(\omega) \tilde{\mathbf{G}}_{\boldsymbol{\psi}'\boldsymbol{\psi}'}(\omega) \tilde{\mathbf{G}}_{\boldsymbol{\psi}'\boldsymbol{\phi}}^{-1}(\omega) - \tilde{\mathbf{G}}_{\boldsymbol{\phi}\boldsymbol{\phi}}^{-1}(\omega), \quad (35)$$

with  $\tilde{\mathbf{G}}^{-1}(\omega) = \mathbf{Q}^\top \mathbf{G}^{-1}(\omega) \mathbf{Q}$  and

$$\mathbf{Q} = \begin{bmatrix} \mathbf{Q}_{\varphi\psi} & \mathbf{Q}_{\varphi\psi'} & 0 & 0 & 0 & 0 \\ 0 & 0 & 1 & 0 & 0 & 0 \\ 0 & 0 & 0 & \mathbf{Q}_{\varphi\psi} & \mathbf{Q}_{\varphi\psi'} & 0 \\ 0 & 0 & 0 & 0 & 0 & 1 \end{bmatrix}. \quad (36)$$

### C. Analytical properties of the self-energy

The self-energy is a meromorphic matrix function of complex-valued frequency. We can classify its poles into two categories. The first category of poles corresponds to the frequencies  $\omega_k^d$  where the matrix  $\tilde{\mathbf{G}}_{\boldsymbol{\psi}'\boldsymbol{\psi}'}(\omega)$  is singular. They have a purely classical origin and we refer to them as dynamical poles. Since these poles come from a matrix inverse, the corresponding residues have unit rank. The other category of poles arise from the Bose-Einstein distribution function  $\coth[\hbar\omega/(2k_B T)]$  and corresponds to bosonic Matsubara frequencies  $i\omega_n^m = 2\pi n k_B T/\hbar$ ,  $n = \pm 1, \pm 2, \dots$ . Since all dynamical variables and source fields are real-valued in the time domain, the self-energy has the symmetry property  $\boldsymbol{\Sigma}_{\text{core}}(t) = \boldsymbol{\Sigma}_{\text{core}}^\top(-t)$ . Hence the action  $S_{\text{core}}[\boldsymbol{\phi}_{\text{core}}]$  can be expressed through a modified self-energy with a retarded causality. Due to this symmetry property

$$\int_{-\infty}^{+\infty} \mathbf{y}^\dagger(\omega) \boldsymbol{\Sigma}_{\text{core}}^R(\omega) \mathbf{x}(\omega) d\omega = \int_{-\infty}^{+\infty} \mathbf{x}^\dagger(\omega) \boldsymbol{\Sigma}_{\text{core}}^A(\omega) \mathbf{y}(\omega) d\omega, \quad (37)$$

where  $\mathbf{x}(\omega)$  and  $\mathbf{y}(\omega)$  are Fourier images of arbitrary real-valued vector functions, the advanced component of self-energy can be replaced with the retarded one. We apply a Hilbert transformation to the Keldysh component

$$\tilde{\Sigma}_{\text{core}}^{\text{K}}(\omega) = \frac{\imath}{2\pi} \int_{-\infty}^{+\infty} \frac{\Sigma_{\text{core}}^{\text{K}}(\omega - \omega')}{\omega' + \imath 0^+} d\omega'. \quad (38)$$

The resulted  $\tilde{\Sigma}_{\text{core}}^{\text{K}}(\omega)$  has a retarded causality. It means that all of the poles of  $\tilde{\Sigma}_{\text{core}}^{\text{K}}(\omega)$  are located in the lower complex half-plane and coincide with the poles of  $\Sigma_{\text{core}}^{\text{K}}(\omega)$ . Then we construct a rectangular self-energy matrix

$$\tilde{\Sigma}_{\text{core}}(\omega) = [\Sigma_{\text{core}}^{\text{R}}(\omega) \quad \tilde{\Sigma}_{\text{core}}^{\text{K}}(\omega)] \quad (39)$$

which satisfies

$$\begin{aligned} & \frac{1}{2} \int_{-\infty}^{+\infty} [\mathbf{x}^\dagger(\omega) \quad \mathbf{y}^\dagger(\omega)] \Sigma_{\text{core}}(\omega) \begin{bmatrix} \mathbf{x}(\omega) \\ \mathbf{y}(\omega) \end{bmatrix} d\omega \\ &= \int_{-\infty}^{+\infty} \mathbf{y}^\dagger(\omega) \tilde{\Sigma}_{\text{core}}(\omega) \begin{bmatrix} \mathbf{x}(\omega) \\ \mathbf{y}(\omega) \end{bmatrix} d\omega. \end{aligned} \quad (40)$$

A meromorphic function allows the Mittag-Leffler expansion which has the following form for the self-energy:

$$\tilde{\Sigma}_{\text{core}}(\omega) = \mathbf{P}(\omega) + \sum_k \frac{\mathbf{R}_k^{\text{d}}}{\omega - \omega_k^{\text{d}}} + \sum_n \frac{[0 \quad \mathbf{R}_n^{\text{m}}]}{\omega + \omega_n^{\text{m}}}, \quad (41)$$

where  $\mathbf{P}(\omega) = \mathbf{P}^{(0)} + \mathbf{P}^{(1)}\omega + \mathbf{P}^{(2)}\omega^2$  is a polynomial matrix,  $\mathbf{R}_k^{\text{d}}$  is a unit rank matrix residue at the dynamical pole  $k$ , and  $\mathbf{R}_n^{\text{m}}$  is a matrix residue at the Matsubara pole  $n$  which contributes only to the Keldysh component of the self-energy.

In connection to the above expansion, we note that a sharp cut-off of the Matsubara series gives a quite poor approximation for the cotangent function present in the Bose-Einstein distribution function. In practice it is more efficient to use a rational approximation in the form

$$\coth\left(\frac{\hbar\omega}{2k_{\text{B}}T}\right) \approx \omega\tau + \frac{2k_{\text{B}}T}{\hbar\omega} + \sum_{n=1}^N \frac{2\omega r_n^{\text{gm}}}{\omega^2 + (\omega_n^{\text{gm}})^2}, \quad (42)$$

where  $\omega_n^{\text{gm}}$  are the poles of rational approximations,  $r_n^{\text{gm}}$  are corresponding residues, and  $\tau$  is a constant parameter. Such an approximation can be obtained, e.g., with the symmetrized version of AAA algorithm [47, 75, 86] which turns out to be very accurate in a finite range of frequencies even with very few poles taken into account. We refer to the frequencies  $\omega_n^{\text{gm}}$  as generalized Matsubara frequencies.

Finally, the action for the circuit reads as

$$\begin{aligned} S_{\text{core}}[\phi_{\text{core}}] &= S_{\text{J}}[\psi_{\text{c}}, \psi_{\text{q}}] \\ &+ \int_{-\infty}^{+\infty} \sum_{jj'=0}^1 \frac{d^j \phi_{\text{core,q}}^\top(t)}{dt^j} \mathbf{A}^{(jj')} \frac{d^{j'} \phi_{\text{core}}(t)}{dt^{j'}} dt \\ &- \frac{1}{2\pi} \int_{-\infty}^{+\infty} \sum_k \phi_{\text{core,q}}^\dagger(\omega) \frac{\mathbf{R}_k^{\text{d}}}{\omega - \omega_k^{\text{d}}} \phi_{\text{core}} d\omega \\ &- \frac{1}{2\pi} \int_{-\infty}^{+\infty} \sum_n \phi_{\text{core,q}}^\dagger(\omega) \frac{\mathbf{R}_n^{\text{gm}}}{\omega + i\omega_n^{\text{gm}}} \phi_{\text{core,q}}(\omega) d\omega, \end{aligned} \quad (43)$$

where the influence functional in Eq. (34) has been replaced by the three terms following  $S_{\text{J}}[\psi_{\text{c}}, \psi_{\text{q}}]$ . Here

$$\begin{aligned} \mathbf{A}^{(00)} &= -\mathbf{P}^{(0)}, \\ \mathbf{A}^{(01)} - \mathbf{A}^{(10)} &= -\imath \mathbf{P}^{(1)}, \\ \mathbf{A}^{(11)} &= -\mathbf{P}^{(2)}, \end{aligned} \quad (44)$$

sum  $\mathbf{A}^{(01)} + \mathbf{A}^{(10)}$  can be arbitrary, and  $\mathbf{R}_n^{\text{gm}}$  are the matrix residues at generalized Matsubara poles. We have denoted the quantum components of the vector  $\phi_{\text{core}}$  as  $\phi_{\text{core,q}} = [\psi_{\text{q}}^\top \quad \eta_{\text{o}}^\top]^\top$ .

#### D. Auxiliary modes

We treat each non-local term in the action separately introducing auxiliary bosonic degrees of freedom via the Hubbard-Stratonovich transformation [47, 87, 88] as

$$\begin{aligned} & \exp \left[ -\frac{\imath}{2\pi\hbar} \int_{-\infty}^{+\infty} \mathbf{y}^\dagger(\omega) \frac{\mathbf{R}}{\omega - \omega_*} \mathbf{x}(\omega) d\omega \right] \\ &= \int \mathcal{D}[\mathbf{a}, \mathbf{a}^\dagger] \exp \left\{ \frac{\imath}{\hbar} \int_{-\infty}^{+\infty} [\imath\hbar \mathbf{a}^\dagger(t) \dot{\mathbf{a}}(t) - \hbar\omega_* |\mathbf{a}(t)|^2 \right. \\ & \quad \left. + \mathbf{a}^\dagger(t) \mathbf{V}^\top \mathbf{x}(t) + \mathbf{y}^\top(t) \mathbf{U} \mathbf{a}(t) \right] dt \Big\}, \end{aligned} \quad (45)$$

where  $\mathbf{x}(t)$  and  $\mathbf{y}(t)$  are arbitrary real valued-vector functions,  $\mathbf{R}$  is an arbitrary matrix which is factorized as  $\mathbf{R} = \hbar \mathbf{U} \mathbf{V}^\top$ , and  $\mathbf{a}$  is an auxiliary complex-valued vector degree of freedom. Such a factorization is favorable since the matrix  $\mathbf{R}$  is not full-rank, and can be obtained, e.g., using the singular value decomposition. The dimension of the auxiliary vector degree of freedom  $\mathbf{a}$  is given by the rank of the matrix  $\mathbf{R}$ . Consequently, we obtain a time-local action of the QD-MESS equation as

$$\begin{aligned} S_{\text{QD-MESS}}[\phi_{\text{core}}, \mathbf{a}, \mathbf{b}] &= \int_{-\infty}^{+\infty} \mathcal{L}_{\text{QD-MESS}}(\dot{\phi}_{\text{core}}, \dot{\mathbf{a}}, \dot{\mathbf{b}}, \phi_{\text{core}}, \mathbf{a}, \mathbf{b}) dt, \end{aligned} \quad (46)$$

where the QD-MESS Lagrangian is given by

$$\begin{aligned}
\mathcal{L}_{\text{QD-MESS}} & \left( \dot{\phi}_{\text{core}}, \dot{\mathbf{a}}, \dot{\mathbf{b}}, \phi_{\text{core}}, \mathbf{a}, \mathbf{b} \right) \\
& = -V_{\text{J}}(\psi_{\text{c}}, \psi_{\text{q}}) + \sum_{jj'=0}^1 \frac{d^j \phi_{\text{core,q}}^{\text{T}}}{dt^j} \mathbf{A}^{(jj')} \frac{d^{j'} \phi_{\text{core}}}{dt^{j'}} \\
& \quad + \sum_k \left( i\hbar a_k^* \dot{a}_k - \hbar \omega_k^{\text{d}} |a_k|^2 \right) \\
& \quad + \phi_{\text{core,q}}^{\text{T}} \mathbf{u}_k^{\text{d}} a_k + a_k^* \mathbf{v}_k^{\text{dT}} \phi_{\text{core}} \\
& \quad + \sum_n \left( i\hbar \mathbf{b}_n^{\dagger} \dot{\mathbf{b}}_n + i\omega_n^{\text{gm}} |\mathbf{b}_n|^2 \right) \\
& \quad + \phi_{\text{core,q}}^{\text{T}} \mathbf{U}_n^{\text{gm}} \mathbf{b}_n + \mathbf{b}_n^{\dagger} \mathbf{V}_n^{\text{gmT}} \phi_{\text{core,q}}, \quad (47)
\end{aligned}$$

where  $\mathbf{R}_k^{\text{d}} = \hbar \mathbf{u}_k^{\text{d}} \mathbf{v}_k^{\text{dT}}$ ,  $\mathbf{R}_n^{\text{gm}} = \hbar \mathbf{U}_n^{\text{gm}} \mathbf{V}_n^{\text{gmT}}$ ,  $a_k$  and  $\mathbf{b}_n$  are auxiliary degrees of freedom corresponding to dynamical and Matsubara poles of the self-energy, and all the dynamical variables and sources are given in the time domain. In this Lagrangian all the auxiliary bosonic modes are coupled to the flux degrees of freedom  $\psi_{\text{c}}$  and  $\psi_{\text{q}}$ , hence we refer to the QD-MESS equation produced by this Lagrangian as flux QD-MESS. However, this form is not unique. Instead of applying a Hubbard–Stratonovich transformation as in Eq. (45), we may expand in the integrand

$$\begin{aligned}
\frac{1}{\omega - \omega_*} & = -\frac{1}{\omega_*} + \frac{\omega}{\omega_*(\omega - \omega_*)} = \\
& \quad -\frac{1}{\omega_*} - \frac{\omega}{\omega_*^2} + \frac{\omega^2}{\omega_*^2(\omega - \omega_*)}. \quad (48)
\end{aligned}$$

Multiplication by  $\omega$  of a Fourier image corresponds to applying the  $i\partial_t$  operator in time domain. Hence we can express the time non-local term as

$$\begin{aligned}
& \exp \left[ -\frac{i}{2\pi\hbar} \int_{-\infty}^{+\infty} \mathbf{y}^{\dagger}(\omega) \frac{\mathbf{R}}{\omega - \omega_*} \mathbf{x}(\omega) d\omega \right] \\
& = \int \mathcal{D}[\mathbf{a}, \mathbf{a}^{\dagger}] \exp \left\{ \frac{i}{\hbar} \int_{-\infty}^{+\infty} [i\hbar \mathbf{a}^{\dagger}(t) \dot{\mathbf{a}}(t) \right. \\
& \quad + \hbar \omega_* |\mathbf{a}(t)|^2 + \mathbf{y}^{\text{T}}(t) \mathbf{R} \left( \frac{1}{\omega_*} + \frac{i\partial_t}{\omega_*^2} \right) \mathbf{x}(t) \\
& \quad \left. + \mathbf{a}^{\dagger}(t) \mathbf{V}^{\text{T}} \dot{\mathbf{x}}(t) + \dot{\mathbf{y}}^{\text{T}}(t) \mathbf{U} \mathbf{a}(t) \right] dt \}. \quad (49)
\end{aligned}$$

This way, with a proper renormalization of the time-local terms in the action (43), one can obtain a QD-MESS Lagrangian where the auxiliary degrees of freedom couple to the voltages  $\dot{\psi}_{\text{c}}$  and  $\dot{\psi}_{\text{q}}$  for some of the modes (see Appendix A for details). This formulation may be beneficial for practical calculations, but for the sake of simplicity of the presentation, we proceed with the flux QD-MESS Lagrangian.

## E. QD-MESS equation

To derive the quantum equation which corresponds to the Lagrangian (47), we proceed with a standard transition to the Schrödinger picture. First, we introduce the canonical conjugate variables to the fluxes, i.e., the charges

$$\begin{aligned}
q_{\text{c}} & = \frac{\partial \mathcal{L}_{\text{QD-MESS}}}{\partial \dot{\psi}_{\text{c}}^{\text{T}}}, \\
q_{\text{q}}^{\text{T}} & = \frac{\partial \mathcal{L}_{\text{QD-MESS}}}{\partial \dot{\psi}_{\text{q}}}, \quad (50)
\end{aligned}$$

Then, we apply the Legendre transformation associated with Eq. (50) and obtain the Liouvillian

$$\mathcal{L} = q_{\text{q}}^{\text{T}} \dot{\psi}_{\text{c}} + \dot{\psi}_{\text{q}}^{\text{T}} q_{\text{c}} + i\hbar \sum_k a_k^* \dot{a}_k + i\hbar \sum_n \mathbf{b}_n^{\dagger} \dot{\mathbf{b}}_n - \mathcal{L}_{\text{QD-MESS}}. \quad (51)$$

This Liouvillian, when written as a function of canonical variables, can be interpreted as a quantum Liouvillian by imposing the canonical commutation relations

$$\begin{aligned}
[\check{\psi}_{\text{c},\alpha}, \check{q}_{\text{q},\alpha'}] & = i\hbar \delta_{\alpha\alpha'}, \quad [\check{\psi}_{\text{q},\alpha}, \check{q}_{\text{c},\alpha'}] = i\hbar \delta_{\alpha\alpha'}, \\
[\check{a}_k, \check{a}_{k'}^{\dagger}] & = \delta_{kk'}, \quad [\check{\mathbf{b}}_{n,\alpha}, \check{\mathbf{b}}_{n',\alpha'}^{\dagger}] = \delta_{nn'} \delta_{\alpha\alpha'}, \quad (52)
\end{aligned}$$

with all other single-operator commutators vanishing. Finally, the quantum Liouvillian, which governs the dynamics of the superconducting quantum circuit, reads

$$\begin{aligned}
\check{\mathcal{L}} & = \check{\mathbf{x}}_{\text{q}}^{\text{T}} \mathbf{L}_{\text{quad}} \check{\mathbf{x}} + V_{\text{J}}(\check{\psi}_{\text{c}}, \check{\psi}_{\text{q}}) \\
& \quad + \sum_j \left( \hbar \omega_k^{\text{d}} \check{a}_k^{\dagger} \check{a}_k - \check{a}_k^{\dagger} \mathbf{v}_k^{\text{dT}} \check{\phi}_{\text{core}} - \check{\phi}_{\text{core,q}}^{\text{T}} \mathbf{u}_k^{\text{d}} \check{a}_k \right) \\
& \quad - \sum_n \left( i\hbar \omega_n^{\text{gm}} \check{\mathbf{b}}_n^{\dagger} \check{\mathbf{b}}_n + \check{\mathbf{b}}_n \mathbf{V}_n^{\text{gmT}} \check{\phi}_{\text{core,q}} + \check{\phi}_{\text{core,q}}^{\text{T}} \mathbf{U}_n^{\text{gm}} \check{\mathbf{b}}_n \right), \quad (53)
\end{aligned}$$

where  $\mathbf{L}_{\text{quad}}$  is a constant matrix, which describes the coupling between the classical and the quantum charge and flux operators and their coupling to the sources,  $\check{\mathbf{x}} = [\check{\mathbf{q}}_{\text{c}}^{\text{T}} \ \check{\psi}_{\text{c}}^{\text{T}} \ \dot{\mathbf{v}}_{\text{i}}^{\text{T}} \ \mathbf{v}_{\text{i}}^{\text{T}} \ \check{\mathbf{q}}_{\text{q}}^{\text{T}} \ \check{\psi}_{\text{q}}^{\text{T}} \ \dot{\boldsymbol{\eta}}_{\text{o}}^{\text{T}} \ \boldsymbol{\eta}_{\text{o}}^{\text{T}}]^{\text{T}}$  is a vector of all charges, fluxes, and sources, while  $\check{\mathbf{x}}_{\text{q}} = [\check{\mathbf{q}}_{\text{q}}^{\text{T}} \ \check{\psi}_{\text{q}}^{\text{T}} \ \dot{\boldsymbol{\eta}}_{\text{o}}^{\text{T}} \ \boldsymbol{\eta}_{\text{o}}^{\text{T}}]^{\text{T}}$  is its quantum component,  $\check{\phi}_{\text{core}} = [\check{\psi}_{\text{c}}^{\text{T}} \ \mathbf{v}_{\text{i}}^{\text{T}} \ \check{\psi}_{\text{q}}^{\text{T}} \ \boldsymbol{\eta}_{\text{o}}^{\text{T}}]^{\text{T}}$  is a vector of all fluxes and sources, and  $\check{\phi}_{\text{core,q}} = [\check{\psi}_{\text{q}}^{\text{T}} \ \boldsymbol{\eta}_{\text{o}}^{\text{T}}]^{\text{T}}$  is its quantum component. Note that the ordering of the operators is such that the operators corresponding to the quantum degrees of freedom lie at the left, similarly to the creation operators of the auxiliary bosonic modes. The obtained Liouvillian by its form resembles a Hamiltonian of a bosonic impurity problem, where a nonlinear impurity is coupled to a continuum of harmonic modes. The most studied case in this context is the paradigmatic spin-boson problem [4]. An important difference to the situation is though that here the harmonic modes are discrete and have complex frequencies and couplings.

The QD-MESS equation, which governs the dynamics of the dissipative quantum-electric circuit, reads as

$$i\hbar \frac{d}{dt} |W\rangle = \check{\mathcal{L}}|_{\boldsymbol{\eta}_o=0} |W\rangle, \quad (54)$$

where  $|W\rangle$  is a multidimensional vector in an extended Liouville space, which completely describes a state of both system and its environment. Equation (54) has a conservation law

$$\langle 1 | \frac{d}{dt} |W\rangle = 0, \quad (55)$$

where  $\langle 1 |$  is a left zero eigenvector of the quantum operators of all dynamical variables  $\check{\psi}_q$  and  $\check{q}_q$ , and of the creation operators  $\check{a}^\dagger$  and  $\check{b}^\dagger$  of all the auxiliary modes, i.e. it corresponds to zero occupation number of each of these modes. Consequently, the proper ordering of the operators in the quantum Liouvillian (53) results in

$$\langle 1 | \check{\mathcal{L}}|_{\boldsymbol{\eta}_o=0} = 0. \quad (56)$$

The product  $\langle 1 | W \rangle$  is equivalent to the trace operation of the full system-environment density operator, hence Eq. (55) is equivalent to the conservation of probability for the standard Liouville–von Neumann equation. Thus, it is natural to choose a normalization of both  $|W\rangle$  and  $\langle 1 |$  such that  $\langle 1 | W \rangle = 1$ . The thermal equilibrium state corresponds to a right zero eigenvector of the Liouvillian in the absence of classical and quantum sources fields

$$\check{\mathcal{L}}|_{\boldsymbol{\varphi}_i=0, \boldsymbol{\eta}_o=0} |W_{\text{eq}}\rangle = 0. \quad (57)$$

The physical meaning of the components of  $|W\rangle$  may be non-trivial to identify, especially given that the choice of the degrees of freedom included in the system and in the environment may be arbitrary. This raises two issues: the preparation of the initial state for the simulations and the calculation of the probability distribution of observables. The first issue can be overcome by an explicit simulation of the initialization pulse, assuming the initial state to be the equilibrium state  $|W_{\text{eq}}\rangle$ . Below, we introduce a method how to calculate mutual quasiprobability distributions of various observables.

## F. Observables

Let us focus on a case where we apply an input field and measure the output field within a time interval  $(t^i, t^f)$ . Before  $t^i$ , the open system is in the thermal state  $|W_{\text{eq}}\rangle$ . The result of a measurement is a time trace of the output field  $\mathbf{v}_o(t)$  sampled from a stochastic process. The observables  $\mathbf{o}$  we are interested in are weighted averages of these fields over the above-mentioned time interval, and hence given by

$$\mathbf{o} = \int_{t^i}^{t^f} \mathbf{F}(t) \mathbf{v}_o(t) dt, \quad (58)$$

where  $\mathbf{F}(t)$  is a matrix-valued weight function. Since the output field is stochastic, these observables  $\mathbf{o}$  are random variables. Their mutual quasiprobability distribution can be formally found as [11]

$$p(\mathbf{o}) = \left\langle \delta \left[ -i\hbar \int_{t^i}^{t^f} \mathbf{F}(t) \frac{\delta}{\delta \boldsymbol{\eta}_o^\dagger(t)} dt - \mathbf{o} \right] \mathcal{Z}[\mathbf{v}_i, \boldsymbol{\eta}_o] \right\rangle_{\boldsymbol{\eta}_o=0}, \quad (59)$$

where the argument of the delta function is a linear functional acting on the generating functional  $\mathcal{Z}[\mathbf{v}_i, \boldsymbol{\eta}_o]$ . The latter itself can be calculated by solving the QD-MESS equation (54) with a non-zero quantum source

$$\mathcal{Z}[\mathbf{v}_i, \boldsymbol{\eta}_o] = \langle 1 | \mathbb{T} \exp \left[ -\frac{i}{\hbar} \int_{t^i}^{t^f} \check{\mathcal{L}}(t) dt \right] |W_{\text{eq}}\rangle, \quad (60)$$

where  $\mathbb{T}$  is a time-ordering symbol. By employing a Fourier transformation of a multidimensional delta function, we find that the quasiprobability density can be calculated as

$$p(\mathbf{o}) = \int e^{i\mathbf{s}^\top \mathbf{o}} \mathcal{Z}[\mathbf{v}_i, \hbar \mathbf{F}^\top(t) \mathbf{s}] \frac{d\mathbf{s}}{(2\pi)^{\dim(\mathbf{o})}}. \quad (61)$$

Since  $\mathcal{Z}[\mathbf{v}_i, 0] = 1$  for an arbitrary drive field  $\mathbf{v}_i$ , the quasiprobability density  $p(\mathbf{o})$  integrates to unity. However, it is not clear at this point whether it satisfies the non-negativity requirement for a probability density. For example, the Wigner quasiprobability function, which may have negative values, falls into this class of distribution functions if one chooses  $\mathbf{q}_c$  and  $\boldsymbol{\psi}_c$  as observables instead of the time-averaged output fields.

## IV. WEAK-COUPLING REGIME

Even though it is possible to write a time-local equation of motion which fully describes the dynamics of the dissipative quantum circuit, solving this equation remains challenging due to the exponentially high dimension of the state vector  $|W\rangle$ . This issue is pronounced in the ultra-low temperature domain, where the generalized Matsubara frequencies accumulate to zero.

Curiously, the QD-MESS equation written explicitly in Fock basis of the auxiliary modes, is identical to HEOM [47, 75] which can be solved using tensor network algorithms [89, 90]. Here, we suggest a systematic approach to eliminate weakly coupled auxiliary modes, which results in a substantial reduction of dimensionality required for the Liouville space of linear degrees of freedom. The general form of the QD-MESS Liouvillian reads as

$$\check{\mathcal{L}}(t) = \check{\mathcal{L}}^{(0)}(t) + \sum_k \left\{ [\check{x}'_k + \alpha'_k(t)] \check{a}_k + [\check{x}''_k + \alpha''_k(t)] \check{a}_k^\dagger + \hbar \omega_k \check{a}_k^\dagger \check{a}_k \right\}, \quad (62)$$

where we denote the Liouvillian of all non-linear degrees of freedom as  $\check{\mathcal{L}}^{(0)}(t)$ , unify the dynamical and generalized Matsubara modes, denote all the coupling operators as  $\check{x}'_k$  and  $\check{x}''_k$ , and introduce the drive variables  $\alpha'_k(t)$  and  $\alpha''_k(t)$  which may originate from both, classical  $\mathbf{v}_i$  and quantum  $\boldsymbol{\eta}_o$  sources. Note that this form is not unique since one can incorporate some of the auxiliary modes to  $\check{\mathcal{L}}^{(0)}(t)$ .

First, we eliminate time-dependent source terms by carrying out a shift transformation

$$|W\rangle = e^{\check{T}(t)}|W_{\text{shift}}\rangle, \quad (63)$$

where  $\check{T}(t) = \sum_k \left[ \beta'_k(t)\check{a}_k + \beta''_k(t)\check{a}_k^\dagger \right]$  and the time-dependent shifts  $\beta'_k(t)$  and  $\beta''_k(t)$  are required to satisfy the differential equations

$$\begin{aligned} i\hbar\dot{\beta}'_k(t) &= -\hbar\omega_k\beta'_k(t) + \alpha'_k(t), \\ i\hbar\dot{\beta}''_k(t) &= \hbar\omega_k\beta''_k(t) + \alpha''_k(t). \end{aligned} \quad (64)$$

Thus, the dynamics of  $|W_{\text{shift}}\rangle$  is governed by the following Liouvillian

$$\check{\mathcal{L}}_{\text{shift}}(t) = \check{\mathcal{L}}_{\text{shift}}^{(0)}(t) + \sum_k \left( \check{x}'_k\check{a}_k + \check{x}''_k\check{a}_k^\dagger + \hbar\omega_k\check{a}_k^\dagger\check{a}_k \right), \quad (65)$$

$$\begin{aligned} \check{\mathcal{L}}_{\text{shift}}^{(0)}(t) &= \check{\mathcal{L}}^{(0)}(t) + \sum_k \left[ \check{x}'_k(t)\beta''_k(t) - \check{x}''_k(t)\beta'_k(t) \right] \\ &+ \frac{1}{2} \sum_k \left[ \alpha'_k(t)\beta''_k(t) - \alpha''_k(t)\beta'_k(t) \right]. \end{aligned} \quad (66)$$

Up to this point, we have not done any approximations to arrive at the above Liouvillian since the shift transformation is exact. Next, we proceed with eliminating the transverse coupling to the auxiliary modes by a dynamical Schrieffer–Wolf transformation [78, 79]

$$|W_{\text{shift}}\rangle = e^{\check{S}(t)}|W_{\text{SW}}\rangle, \quad (67)$$

where  $\check{S}(t) = \sum_k \left[ \check{p}'_k(t)\check{a}_k + \check{p}''_k(t)\check{a}_k^\dagger \right]$  and operators  $\check{p}'_k(t)$  and  $\check{p}''_k(t)$  act in the space of the Liouvillian  $\check{\mathcal{L}}_{\text{shift}}^{(0)}(t)$ . We emphasize that this Schrieffer–Wolf transformation is performed at the Liouvillian level and is non-unitary. The first-order expansion of the exponents with respect to operators  $\check{p}'_k(t)$  and  $\check{p}''_k(t)$  reveals that the transverse coupling may be eliminated if  $\check{p}'_k(t)$  and  $\check{p}''_k(t)$  satisfy the following equations:

$$\begin{aligned} i\hbar\frac{d\check{p}'_k(t)}{dt} &= \left[ \check{\mathcal{L}}_{\text{shift}}^{(0)}(t), \check{p}'_k(t) \right] - \hbar\omega_k\check{p}'_k(t) + \check{x}'_k, \\ i\hbar\frac{d\check{p}''_k(t)}{dt} &= \left[ \check{\mathcal{L}}_{\text{shift}}^{(0)}(t), \check{p}''_k(t) \right] + \hbar\omega_k\check{p}''_k(t) + \check{x}''_k. \end{aligned} \quad (68)$$

TABLE I. Parameters of the circuit shown in Fig. 2 used for numerical calculations.

$C_t$	$E_J/h$	$C_r$	$L_r$	$C_c$	$C_o$	$Z$
80 fF	12.5 GHz	570 fF	0.7 nH	40 fF	15 fF	50 $\Omega$

The second-order expansion yields the Schrieffer–Wolf correction to the Liouvillian

$$\check{\mathcal{L}}_{\text{SW}} \approx \check{\mathcal{L}}_{\text{shift}}^{(0)}(t) + \sum_k \left\{ \hbar\omega_k\check{a}_k^\dagger\check{a}_k + \frac{1}{2} \left[ \check{x}'_k\check{a}_k + \check{x}''_k\check{a}_k^\dagger, \check{S}(t) \right] \right\}. \quad (69)$$

Next, we apply a partial rotating-wave approximation for the auxiliary degrees of freedom, keeping only the diagonal terms  $\check{a}_k^\dagger\check{a}_k$ . This results in

$$\begin{aligned} \check{\mathcal{L}}_{\text{SW}}(t) &\approx \check{\mathcal{L}}_{\text{SW}}^{(0)}(t) + \sum_k \left\{ \hbar\omega_k + [\check{x}'_k, \check{p}''_k(t)] \right\} \check{a}_k^\dagger\check{a}_k, \\ \check{\mathcal{L}}_{\text{SW}}^{(0)}(t) &= \check{\mathcal{L}}_{\text{shift}}^{(0)}(t) + \frac{1}{2} \sum_k \left[ \check{x}'_k\check{p}''_k(t) - \check{p}'_k(t)\check{x}''_k \right]. \end{aligned} \quad (70)$$

The last step is valid only if there are no pairs  $(k, k')$  for which  $\omega_k \pm \omega_{k'}$  is small. Such a delicate case appears, for example, for two weakly decaying dynamical modes with frequencies  $\omega_k = -\omega_{k'}^*$ . These pairs should be treated carefully: One may either keep the off-diagonal terms  $\check{a}_k\check{a}_{k'}$  and  $\check{a}_k^\dagger\check{a}_{k'}^\dagger$  in the transformed Liouvillian, or take these modes into account exactly by incorporating them into  $\check{\mathcal{L}}^{(0)}(t)$  in the original Liouvillian (62).

The dynamical Schrieffer–Wolf transformation is perturbative, hence it can be applied only to systems weakly coupled to the auxiliary modes. This perturbative treatment is similar to standard Born–Markov approximations widely used for open quantum systems in a weak coupling regime. However, the presented approach provides a systematic way to derive dissipative terms in the Liouvillian in case of complicated circuits, for which employing the standard IO theory [52–54] becomes hindered. On top of that, resonances can be treated accurately by incorporating weakly decaying auxiliary modes into the Liouvillian  $\check{\mathcal{L}}^{(0)}(t)$ .

In addition to the weak coupling requirement, one of the most restrictive limitations of this approach is that it can be used only for sufficiently small systems, for which Eq. (68) can be solved exactly. This makes it challenging for circuits with multiple Josephson junctions or many weakly decaying dynamical modes. However, accurate solutions of even small circuits may be of great interest, for example, from the point of view of single-qubit operation fidelities.

## V. DISPERSIVE READOUT OF A TRANSMON QUBIT

Here, we demonstrate our theory in an experimentally feasible scenario by applying it to a model of the dis-

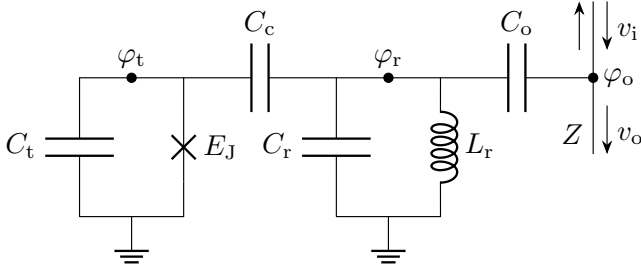


FIG. 2. Schematic of a dispersive readout setup for a transmon qubit. The circuit consists of the qubit, capacitively coupled to a resonator, which in turn capacitively coupled to two semi-infinite transmission lines.

persive readout of a superconducting qubit [51]. As an example system shown in Fig. 2, we employ a typical transmon qubit [91] which is capacitively coupled to an off-resonant readout resonator. The resonator is capacitively coupled to two semi-infinite transmission lines, one of which is used to drive the readout mode and the other to measure the output field. No input is applied on the transmission line for the measurement and the output field to the drive line is disregarded.

Kirchhoff's law for the circuit shown in Fig. 2 yields

$$\begin{aligned}
 -(C_t + C_c) \ddot{\varphi}_t + C_c \ddot{\varphi}_r - \frac{2\pi E_J}{\Phi_0} \sin\left(\frac{2\pi\varphi_t}{\Phi_0}\right) &= 0, \\
 -(C_r + C_c + C_o) \ddot{\varphi}_r + C_c \ddot{\varphi}_t + C_o \ddot{\varphi}_o - \frac{\varphi_r}{L_r} &= 0, \\
 -C_o (\ddot{\varphi}_o - \ddot{\varphi}_r) - \frac{2}{Z} (\dot{\varphi}_o - v_i) &= 0, \\
 v_o &= \dot{\varphi}_o.
 \end{aligned} \tag{71}$$

The blocks of inverse Green's functions (30) for this circuit are given by

$$\begin{aligned}
 \mathbf{K}^R(\omega) &= \begin{bmatrix} \omega^2 \tilde{C}_t & -\omega^2 C_c & 0 & 0 \\ -\omega^2 C_c & \omega^2 \tilde{C}_r - L_r^{-1} & -\omega^2 C_o & 0 \\ 0 & -\omega^2 C_o & \omega^2 C_o + 2i\omega Z^{-1} & 2Z^{-1} \\ 0 & 0 & -i\omega & 0 \end{bmatrix}, \\
 \mathbf{K}^A(\omega) &= [\mathbf{K}^R(\omega^*)]^\dagger, \\
 \mathbf{K}^K(\omega) &= \begin{bmatrix} 0 & 0 & 0 & 0 \\ 0 & 0 & 0 & 0 \\ 0 & 0 & 2i\omega Z^{-1} \coth\left(\frac{\hbar\omega}{2k_B T}\right) & 0 \\ 0 & 0 & 0 & 0 \end{bmatrix},
 \end{aligned} \tag{72}$$

where  $\tilde{C}_t = C_t + C_c$  and  $\tilde{C}_r = C_r + C_c + C_o$ . The dynamical degree of freedom of the core system is represented by transmon flux  $\psi = \varphi_t$ . The rest of the circuit can be described by three dynamical auxiliary modes, two of them have frequencies close to  $\pm 1/\sqrt{L_r \tilde{C}_r}$  with small negative imaginary parts and one with purely imaginary frequency around  $-2i/(ZC_o)$ . For our calculations we use parameters of the circuit shown in Tab. I.

It appears to be more convenient to use coupling to the auxiliary modes through voltage  $\hat{\psi}$  instead of flux

TABLE II. Frequency  $\omega_t$ , linewidth  $\gamma_t$ , and anharmonicity  $\alpha$  of the transmon, frequency  $\omega_r$  and linewidth  $\gamma_r$  of the resonator, and the dispersive shift  $\chi$ , obtained from the diagonalization of the system Liouvillian. The qubit linewidth is given at low (top cell) and high (bottom cell) temperatures. All the quantities are given in GHz.

$\omega_t/(2\pi)$	$\gamma_t/(2\pi)$	$\alpha/(2\pi)$	$\omega_r/(2\pi)$	$\gamma_r/(2\pi)$	$\chi/(2\pi)$
3.834	$10^{-6}$	-0.175	7.719	$1.71 \cdot 10^{-3}$	$-6.4 \cdot 10^{-3}$
	$6.9 \cdot 10^{-5}$				

coupling shown in Eq. (47). This leads to the coupling through the charge of the transmon island to the auxiliary modes in Liouvillian. More details can be found in Appendix A. Since the coupling is weak, we may apply the dynamical Schrieffer–Wolf approach developed in Sec. IV for all of the generalized Matsubara modes and the dynamical mode with imaginary frequency. We restrict the linear space of  $\check{\mathcal{L}}^{(0)}(t)$  and the coupling operators in the Liouvillian (62) to the four lowest levels for the isolated transmon and six levels for the weakly dissipative auxiliary modes. See more technical details on the construction of the Liouvillian in Appendix B.

### A. Transmission coefficient

As the first step we probe the spectrum of the device by calculating the transmission coefficient  $S_{21}(\omega)$ . It is defined as  $\langle v_o(\omega) \rangle = S_{21}(\omega) v_i(\omega)$  for infinitesimal drive  $v_i$ , where the average is taken over the realizations of the output field. It can be evaluated as [11]

$$S_{21}(\omega) = -i\hbar \frac{\delta^2 Z[v_i, \eta_o]}{\delta v_i(\omega) \delta \eta_o^*(\omega)} \Big|_{v_i=0, \eta_o=0}. \tag{73}$$

In order to calculate it, we apply a Schrieffer–Wolf transformation for  $v_i = 0$  and  $\eta_o = 0$  to the static Liouvillian and to the drive terms. The resulting Liouvillian assumes the form

$$\begin{aligned}
 \check{\mathcal{L}}_{\text{SW}} &= \check{\mathcal{L}}_{\text{SW}}^{(\text{static})} \\
 &+ [\eta_o \quad \dot{\eta}_o \quad 1] \begin{bmatrix} L_{oi}^{(00)} & L_{oi}^{(01)} & \check{V}_c^{(0)} \\ L_{oi}^{(10)} & L_{oi}^{(11)} & \check{V}_c^{(1)} \\ \check{V}_q^{(0)} & \check{V}_q^{(1)} & 0 \end{bmatrix} \begin{bmatrix} v_i \\ \dot{v}_i \\ 1 \end{bmatrix}.
 \end{aligned} \tag{74}$$

Here the static Liouvillian is equal to

$$\check{\mathcal{L}}_{\text{SW}}^{(\text{static})} = \check{\mathcal{L}}_{\text{SW}} \Big|_{v_i=0, \eta_o=0}, \tag{75}$$

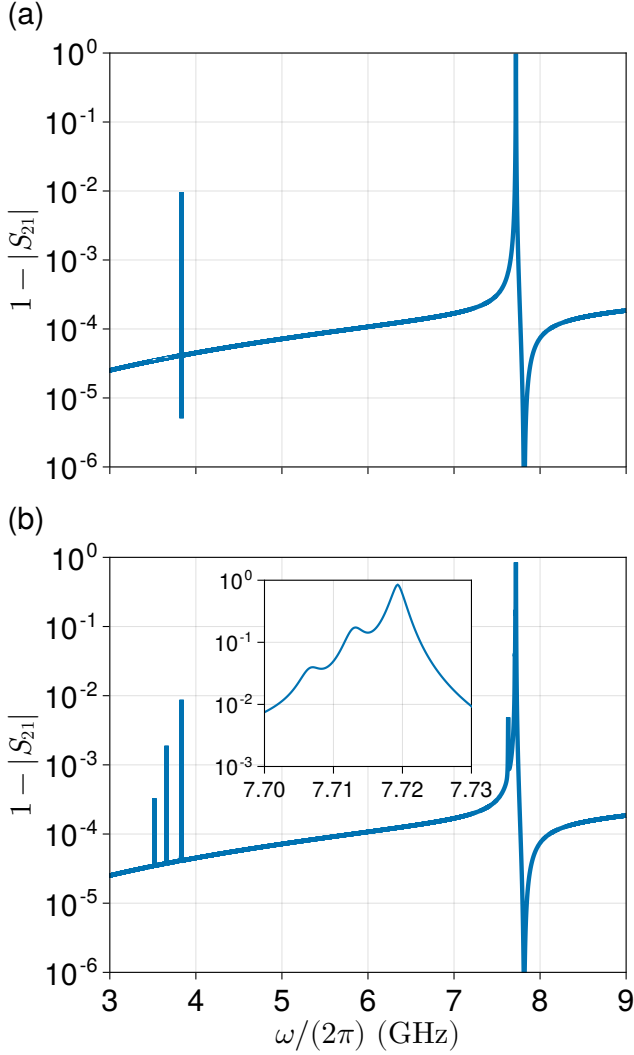


FIG. 3. Absolute value of the transmission coefficient  $S_{21}(\omega)$  for (a) cold transmon at temperature  $T = 0.01$  K and (b) hot transmon at temperature  $T = 0.1$  K. The parameters of the circuit are given in Tab. I. Frequencies and linewidths of the qubit and the resonator, qubit anharmonicity and dispersive shift are shown in Tab. II.

operators which couple system degrees of freedom with the input and output field are given by

$$\begin{aligned}
 \check{V}_c^{(0)} &= \left( \frac{\partial \check{\mathcal{L}}}{\partial \eta_o} + \left[ \frac{\partial \check{\mathcal{L}}}{\partial \eta_o}, \check{S} \right] \right) \Big|_{v_i=0, \eta_o=0}, \\
 \check{V}_c^{(1)} &= \left( \frac{\partial \check{\mathcal{L}}}{\partial \dot{\eta}_o} + \left[ \frac{\partial \check{\mathcal{L}}}{\partial \dot{\eta}_o}, \check{S} \right] \right) \Big|_{v_i=0, \eta_o=0}, \\
 \check{V}_q^{(0)} &= \left( \frac{\partial \check{\mathcal{L}}}{\partial v_i} + \left[ \frac{\partial \check{\mathcal{L}}}{\partial v_i}, \check{S} \right] \right) \Big|_{v_i=0, \eta_o=0}, \\
 \check{V}_q^{(1)} &= \left( \frac{\partial \check{\mathcal{L}}}{\partial \dot{v}_i} + \left[ \frac{\partial \check{\mathcal{L}}}{\partial \dot{v}_i}, \check{S} \right] \right) \Big|_{v_i=0, \eta_o=0},
 \end{aligned} \tag{76}$$

and direct coupling between the input and output field is provided by

$$\begin{aligned}
 L_{oi}^{(00)} &= \frac{\partial^2 \check{\mathcal{L}}}{\partial \eta_o \partial v_i} \Big|_{v_i=0, \eta_o=0}, & L_{oi}^{(01)} &= \frac{\partial^2 \check{\mathcal{L}}}{\partial \eta_o \partial \dot{v}_i} \Big|_{v_i=0, \eta_o=0}, \\
 L_{oi}^{(10)} &= \frac{\partial^2 \check{\mathcal{L}}}{\partial \dot{\eta}_o \partial v_i} \Big|_{v_i=0, \eta_o=0}, & L_{oi}^{(11)} &= \frac{\partial^2 \check{\mathcal{L}}}{\partial \dot{\eta}_o \partial \dot{v}_i} \Big|_{v_i=0, \eta_o=0}.
 \end{aligned} \tag{77}$$

The latter are c-numbers since the both classical and quantum fields couple linearly to the system and auxiliary degrees of freedom in the Liouvillian (53). Here, we drop the terms quadratic in  $\eta_o$ , since they contribute only to the fluctuations. We emphasize that the generator of the Schrieffer–Wolf transformation  $\check{S}$  should be assumed for the absent drive  $v_i = 0$  and  $\eta_o = 0$ .

Then, the transmission coefficient can be expressed as

$$\begin{aligned}
 S_{21}(\omega) &= \sum_{jj'=0}^1 \varrho^{j-j'} \omega^{j+j'} \langle 1 | \check{V}_c^{(j)} \check{\mathfrak{G}}(\omega) \check{V}_q^{(j')} | W_{\text{eq}} \rangle \\
 &\quad + \sum_{jj'=0}^1 \varrho^{j-j'} \omega^{j+j'} L_{oi}^{(jj')}, \tag{78}
 \end{aligned}$$

where  $\check{\mathfrak{G}}(\omega) = [\omega - \check{\mathcal{L}}_{\text{SW}}^{(\text{static})}]^{-1}$  which can be efficiently calculated using numerical diagonalization of the static Liouvillian.

The frequency dependence of the absolute value of  $S_{21}(\omega)$  is shown in Fig. 3 at a low temperature of  $T = 0.01$  K and a high temperature of  $T = 0.1$  K. At the low temperature, the circuit is close to its ground state and there are only two transitions visible. There is a strong feature at the resonator frequency  $\omega_r$  and a weak signature at the transmon frequency  $\omega_t$ . At the high temperature, both qubit and resonator become thermally populated, and consequently more transitions become visible. In Fig. 3(b), we can clearly observe lines which correspond to transitions between different transmon levels as well as the splitting of the resonator feature caused by the dispersive shift (see the inset). A spurious feature below the resonator peak arises due to the hard cut-off of the transmon levels which results in the increased dispersive shift for the highest considered transmon level. Positions of the peaks and their widths correspond to the eigenvalues of the Liouvillian  $\check{\mathcal{L}}_{\text{SW}}^{(\text{static})}$ . The results are shown in Tab. II. Note that the linewidth of the qubit transition is increased at high temperature which would result in the lower  $T_2$  time of the qubit.

## B. Readout of a hot transmon

Next, we proceed to the simulation of the state of the output field during transmon readout. For the sake of simplicity, we do not consider the preparation of the qubit state and the simulation of its subsequent dynamics with

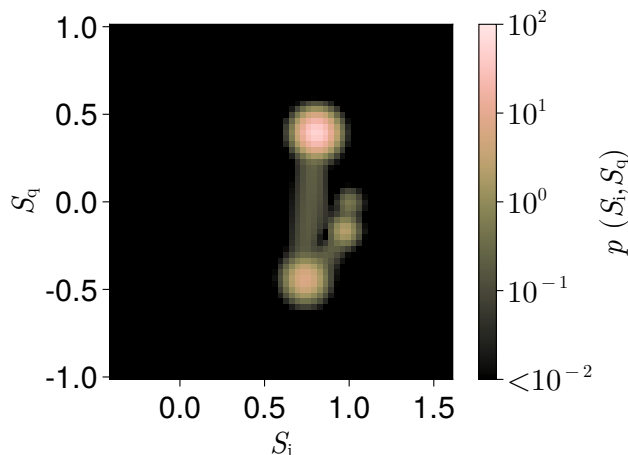


FIG. 4. Quasiprobability density of normalized in-phase and quadrature components of the output field. Temperature is  $T = 0.1$  K, drive frequency is  $\omega_d = 2\pi \times 7.7146$  GHz, drive amplitude is  $V_d = 0.2$   $\mu$ V, integration time is  $t_{\text{int}} = 5.18$   $\mu$ s.

respect to the readout pulse. Instead, we consider a continuous monochromatic drive  $v_i(t) = V_d \cos(\omega_d t)$  and the qubit-resonator system at temperature  $T$  relaxed to the steady state with respect to the drive. Details of the calculation can be found in Appendix C.

The quantity of interest is a homodyne demodulated signal averaged over a finite time interval of length  $t_{\text{int}}$ :

$$S_i + \imath S_q = \frac{2}{t_{\text{int}} V_d} \int_0^{t_{\text{int}}} v_o(t) e^{\imath \omega_d t} dt. \quad (79)$$

The real and imaginary components  $S_i$  and  $S_q$  correspond to in-phase and quadrature components of the output field, respectively, normalized by drive amplitude. These components are measured also in the single-shot readout experiments although typically using a weighted time average over the duration of the readout pulse. We calculate the quasiprobability density  $p(S_i, S_q)$  using Eq. (61) and show the results and simulation parameters in Fig. 4. We can clearly distinguish four disk-shaped clouds which correspond to the different transmon states. The intensities of the clouds are proportional to the thermal populations of the qubit states. In addition there are faint lines which connect different clouds. These lines correspond to the spontaneous transitions between the qubit states which may occur during the integration time [92]. Similar connecting lines have indeed been observed in experiments [93].

The value of  $t_{\text{int}}$  is pivotal for the accurate readout protocol. For long integration times, the spontaneous transitions become more and more probable and in the limit  $t_{\text{int}} \rightarrow \infty$ , the quasiprobability distribution collapses into a delta function centered at the real and imaginary parts of the transmission coefficient for the finite-amplitude drive. In the opposite limit, with the decrease of  $t_{\text{int}}$ , the clouds begin to grow and, at some point, overlap.

Therefore, there is an optimal integration time, not too short such that the clouds can still be distinguishable, and not too long such that probability of spontaneous transition during the measurement is small.

### C. Connection to measurement theory

The choice of the qubit readout problem, in addition to the purely illustrative purpose, is also motivated by the problem of the quantum measurement. The qubit readout falls into a class of continuous inefficient measurements [49] since the state of the qubit is not probed directly, but through the averaging of the output field over a finite time interval. In a contrast to the standard presentation of measurements [49], we do not consider an initial product state of the system and the environment or the measurement device, but a thermal initial state. Moreover, we do not separate the system and the environment and study the open quantum system as a whole. Such an approach may be favorable outside of the weak coupling regime, where product initial states gives rise to non-exponential short-time decoherence [94, 95].

## VI. CONCLUSIONS

We presented an exact nonlinear response theory, free of the limiting requirements of weak coupling, low temperature, and weak drive. The dissipation and the driving field introduced by the coupled transmission lines is reduced to the coupling of the non-linear system degrees of freedom to a discrete set of auxiliary bosonic modes. We split the modes into two classes: dynamical and generalized Matsubara modes. The first ones provide coupling to classical field, while latter are responsible for thermal and quantum fluctuations in the circuit. This results in the emergence of a time-local QD-MESS equation which fully describes the open-quantum-system dynamics of the circuit.

We introduced observables as weighted time averages of the output fields emitted to the transmission lines and derived an analytical expression of their mutual quasiprobability distribution based on the Fourier transformation of the generating functional. This formalism allows to calculate homo- and heterodyne demodulated signal as well as calculate broadband characteristics of the output field.

In the weak coupling regime, we employed a dynamical Schrieffer–Wolf transformation, which provides a consistent way of calculating the dissipators for arbitrary circuits and driving fields. Finally, we illustrated our findings by studying a dispersive-readout setup of a superconducting transmon qubit.

The developed NLR theory provides a powerful framework for the theoretical analysis of open quantum systems such as superconducting quantum circuits, including extraction of experimentally observable quantities.

Going beyond the weak-coupling regime can be achieved by solving the QD-MESS equation with advanced numerical techniques such as tensor networks. In principle, the developed formalism can be applied not only to lumped-element circuits but also to distributed elements. The necessary self-energies can be computed explicitly using high-frequency simulation software for linear components of the distributed element circuits. This would pave the way for exact quantum simulations of practical devices.

In the future, the presented formalism can also be modified for the calculation of thermodynamic properties of the circuit. A non-equilibrium case can be simulated by introducing generalized Matsubara modes corresponding to different temperatures. Here, the counting field corresponding to the heat flow couples to the classical expression for Joule losses which are quadratic in terms of the microwave field in the circuit. Such a generalization would allow to study heat transport in non-equilibrium systems and implement accurate simulations of quantum heat engines.

Among our findings there is a treatment of open quantum systems free from explicit system-environment separation and from an initial product state condition. Such a description is valuable for the development of the measurement theory in the regime of intermediate to strong coupling between the system and the measurement device.

## ACKNOWLEDGMENTS

V.V. thanks Kalle Kansanen and Riya Baruah for fruitful discussions. This work has been financially supported by the Academy of Finland Centre of Excellence program (project no. 336810) and THEPOW (project no. 349594), the European Research Council under Advanced Grant no. 101053801 (ConceptQ), by Horizon Europe programme HORIZON-CL4-2022-QUANTUM-01-SGA via the project 101113946 OpenSuperQPlus100, the German Science Foundation (DFG) under AN336/12-1 (For2724), the State of Baden-Württemberg under KQCBW/SiQuRe, and the BMBF within the QSolid project. We acknowledge the computational resources provided by the Aalto Science-IT project.

### Appendix A: Charge QD-MESS equation

In this appendix, we provide the charge QD-MESS equation in contrast to the flux version considered in the main article. We begin with the classical QD-MESS Lagrangian with the voltage coupling to the auxiliary de-

grees of freedom, given by

$$\begin{aligned} \tilde{\mathcal{L}}_{\text{QD-MESS}} \left( \dot{\phi}_{\text{core}}, \dot{\mathbf{a}}, \dot{\mathbf{b}}, \phi_{\text{core}}, \mathbf{a}, \mathbf{b} \right) = & -V_j(\psi_c, \psi_q) \\ & + \sum_{jj'=0}^1 \frac{d^j \phi_{\text{core,q}}^\top}{dt^j} \tilde{\mathbf{A}}^{(jj')} \frac{d^{j'} \phi_{\text{core}}}{dt^{j'}} \\ & + \sum_k \left( i\hbar a_k^* \dot{a}_k - \hbar \omega_k^{\text{d}} |a_k|^2 \right. \\ & \left. + \tilde{\phi}_{\text{core,q}}^\top \tilde{\mathbf{u}}_k^{\text{d}} a_k + a_k^* \tilde{\mathbf{v}}_k^{\text{d}\top} \tilde{\phi}_{\text{core}} \right) \\ & + \sum_n \left( i\hbar \mathbf{b}_n^\dagger \dot{\mathbf{b}}_n + \omega_n^{\text{gm}} |\mathbf{b}_n|^2 \right. \\ & \left. + \tilde{\phi}_{\text{core,q}}^\top \tilde{\mathbf{U}}_n^{\text{gm}} \mathbf{b}_n + \mathbf{b}_n^\dagger \tilde{\mathbf{V}}_n^{\text{gm}\top} \tilde{\phi}_{\text{core,q}} \right), \quad (\text{A1}) \end{aligned}$$

where  $\tilde{\phi}_{\text{core}} = [\psi_c^\top \ \mathbf{v}_i^\top \ \psi_q^\top \ \boldsymbol{\eta}_o^\top]^\top$  and  $\tilde{\phi}_{\text{core,q}} = [\psi_q^\top \ \boldsymbol{\eta}_o^\top]^\top$ . The expressions for the classical and quantum charges (50), Liouvillian (51) and the commutation relations (52) remain valid but the part of the Liouvillian which describes the dynamics of the auxiliary modes becomes non-diagonal. The form of Eq. (62) can be obtained by applying the Bogoliubov transformation to the operators of the auxiliary modes. The difference from the flux QD-MESS Liouvillian is that the operators of the auxiliary modes are coupled to the charge degrees of freedom.

The main advantage of using the charge QD-MESS equation for the transmon readout circuit shown in Fig. 2 is that it evades spurious inductive terms in the Liouvillian which would break quasi-charge conservation of the transmon island.

### Appendix B: Discrete approximation of QD-MESS for the transmon

Direct numerical simulation of the QD-MESS equation is impossible, since even the Liouvillian  $\tilde{\mathfrak{L}}^{(0)}(t)$  in Eq. (62) is infinite-dimensional and one needs to come up with its finite-dimensional approximation in some suitable basis. For a general circuit with intermediate or strong dissipation it may be a challenging problem. For the transmon readout circuit we use, the coupling of the qubit to the resonator and to the transmission lines is weak, and hence we can use a finite number of bare transmon basis states for our calculations. The dissipation-free part of the transmon Liouvillian reads as

$$\tilde{\mathfrak{L}}_{\text{t}} = \frac{\check{q}_{\text{q}} \check{q}_{\text{c}}}{C_{\text{eff}}} + 2E_j \sin \left( \frac{2\pi \check{\psi}_{\text{c}}}{\Phi_0} \right) \sin \left( \frac{\pi \check{\psi}_{\text{q}}}{\Phi_0} \right). \quad (\text{B1})$$

We make a substitution

$$\begin{aligned} \check{\psi}_{\text{c}} &= \frac{\check{\psi}_+ + \check{\psi}_-}{2}, \quad \check{q}_{\text{c}} = \frac{\check{q}_+ + \check{q}_-}{2}, \\ \check{\psi}_{\text{q}} &= \check{\psi}_+ - \check{\psi}_-, \quad \check{q}_{\text{q}} = \check{q}_+ - \check{q}_-, \end{aligned} \quad (\text{B2})$$

which is a transformation from the classical and quantum variables to the forward and backward-path variables. In terms of these variables, the Liouvillian assumes the form

$$\begin{aligned} \check{\mathcal{L}}_t &= \check{H}_+ - \check{H}_-, \\ \check{H}_\pm &= \frac{\check{q}_\pm^2}{2C_{\text{eff}}} - E_j \cos\left(\frac{2\pi\check{\psi}_\pm}{\Phi_0}\right). \end{aligned} \quad (\text{B3})$$

This Liouvillian is nothing but a commutator with a standard transmon Hamiltonian

$$\begin{aligned} \check{\mathcal{L}}_t \text{vec}(\hat{\rho}) &= \text{vec}\left(\left[\hat{H}, \hat{\rho}\right]\right), \\ \hat{H} &= \frac{\hat{q}^2}{2C_{\text{eff}}} - E_j \cos\left(\frac{2\pi\hat{\psi}}{\Phi_0}\right), \end{aligned} \quad (\text{B4})$$

where  $\text{vec}(\hat{\rho})$  stands for the vectorization of the density operator. For the latter, we can construct a finite-difference approximation, diagonalize it numerically and use a few lowest transmon levels  $|n\rangle$  with energies  $E_n$  as a basis. Consequently, an arbitrary operator  $\hat{A}_\pm$  acting in the Liouville space can be expressed through its counterpart  $\hat{A}$  acting in the Hilbert space as

$$\check{A}_+ \check{\rightarrow} \hat{A} \otimes \hat{1}, \quad \check{A}_- \check{\rightarrow} \hat{1} \otimes \hat{A}^\dagger, \quad (\text{B5})$$

where  $\check{\rightarrow}$  stands for isomorphism relation,  $\otimes$  denotes Kronecker product, and  $\hat{1}$  is the identity operator in the Hilbert space. For the bosonic operators of the auxiliary modes, which we do not eliminate with dynamical Schrieffer–Wolf transformation, we cut the Liouville space with a few lowest levels. For our calculations, we

use four levels of the transmon and six levels of the auxiliary modes.

### Appendix C: QD-MESS equation for the periodically driven system

For the transmon readout we solve the QD-MESS equation with the following classical and quantum sources:

$$\begin{aligned} v_i(t) &= V_d \cos(\omega_d t), \\ \eta_o(s_1, s_2, t) &= s_1 \cos(\omega_d t) + s_2 \sin(\omega_d t), \end{aligned} \quad (\text{C1})$$

for different values of the parameters  $s_1$  and  $s_2$ . The total Liouvillian is periodic in time, and hence Floquet theory can be applied to such a system. We consider the evolution operator over a single period as

$$\check{U}(s_1, s_2) = \mathbb{T} \exp \left[ -\frac{i}{\hbar} \int_0^{2\pi/\omega_d} \check{\mathcal{L}}(t) dt \right]. \quad (\text{C2})$$

The steady state of the system corresponds to the unit eigenstate of this operator in the absence of the quantum drive

$$\check{U}(0)|W_{ss}\rangle = |W_{ss}\rangle. \quad (\text{C3})$$

We consider that the integration time  $t_{\text{int}}$  is an integer multiple  $N$  of the drive period  $2\pi/\omega_d$ . Thus the characteristic function can be evaluated as

$$\mathcal{Z}(s_1, s_2) = \langle 1 | \left[ \check{U}\left(\frac{s_1}{N}, \frac{s_2}{N}\right) \right]^N |W_{ss}\rangle. \quad (\text{C4})$$

These quantities can be efficiently evaluated using the dynamical Schrieffer–Wolf approach for weakly coupled auxiliary modes.

- 
- [1] C. Gardiner and P. Zoller, *Quantum noise: a handbook of Markovian and non-Markovian quantum stochastic methods with applications to quantum optics* (Springer Science & Business Media, 2004).
  - [2] H.-P. Breuer, F. Petruccione, *et al.*, *The theory of open quantum systems* (Oxford University Press on Demand, 2002).
  - [3] U. Weiss, *Quantum dissipative systems* (World Scientific, 2012).
  - [4] A. J. Leggett, S. Chakravarty, A. T. Dorsey, M. P. Fisher, A. Garg, and W. Zwerger, Dynamics of the dissipative two-state system, *Reviews of Modern Physics* **59**, 1 (1987).
  - [5] G. Schön and A. D. Zaikin, Quantum coherent effects, phase transitions, and the dissipative dynamics of ultra small tunnel junctions, *Physics Reports* **198**, 237 (1990).
  - [6] W. H. Zurek, Decoherence, einselection, and the quantum origins of the classical, *Reviews of modern physics* **75**, 715 (2003).
  - [7] M. A. Nielsen and I. L. Chuang, *Quantum computation and quantum information* (Cambridge university press, 2010).
  - [8] D. V. Averin, B. Ruggiero, and P. Silvestrini, *Macroscopic quantum coherence and quantum computing* (Springer Science & Business Media, 2012).
  - [9] A. Beige, D. Braun, B. Tregenna, and P. L. Knight, Quantum computing using dissipation to remain in a decoherence-free subspace, *Physical review letters* **85**, 1762 (2000).
  - [10] F. Verstraete, M. M. Wolf, and J. Ignacio Cirac, Quantum computation and quantum-state engineering driven by dissipation, *Nature physics* **5**, 633 (2009).
  - [11] A. Kamenev, *Field theory of non-equilibrium systems* (Cambridge University Press, 2023).
  - [12] M. O. Scully and M. S. Zubairy, *Quantum optics* (1999).
  - [13] I. Georgescu, 25 years of quantum error correction, *Nature Reviews Physics* **2**, 519 (2020).

- [14] J. Preskill, Quantum computing in the nisq era and beyond, *Quantum* **2**, 79 (2018).
- [15] F. Reiter, A. S. Sørensen, P. Zoller, and C. Muschik, Dissipative quantum error correction and application to quantum sensing with trapped ions, *Nature communications* **8**, 1822 (2017).
- [16] K. Y. Tan, M. Partanen, R. E. Lake, J. Govenius, S. Masuda, and M. Möttönen, Quantum-circuit refrigerator, *Nature communications* **8**, 1 (2017).
- [17] T. Ilias, D. Yang, S. F. Huelga, and M. B. Plenio, Criticality-enhanced quantum sensing via continuous measurement, *PRX Quantum* **3**, 010354 (2022).
- [18] A. Ronzani, B. Karimi, J. Senior, Y.-C. Chang, J. T. Peltonen, C. Chen, and J. P. Pekola, Tunable photonic heat transport in a quantum heat valve, *Nature Physics* **14**, 991 (2018).
- [19] S. Hernández-Gómez, S. Gherardini, N. Staudenmaier, F. Poggiali, M. Campisi, A. Trombettoni, F. Cataliotti, P. Cappellaro, and N. Fabbri, Autonomous dissipative maxwell’s demon in a diamond spin qutrit, *PRX Quantum* **3**, 020329 (2022).
- [20] Q. Bouton, J. Nettersheim, S. Burgardt, D. Adam, E. Lutz, and A. Widera, A quantum heat engine driven by atomic collisions, *Nature Communications* **12**, 2063 (2021).
- [21] A. Redfield, The theory of relaxation processes, in *Advances in Magnetic and Optical Resonance*, Vol. 1 (Elsevier, 1965) pp. 1–32.
- [22] G. Lindblad, On the generators of quantum dynamical semigroups, *Communications in Mathematical Physics* **48**, 119 (1976).
- [23] V. Gorini, A. Kossakowski, and E. C. G. Sudarshan, Completely positive dynamical semigroups of n-level systems, *Journal of Mathematical Physics* **17**, 821 (1976).
- [24] B.-H. Liu, L. Li, Y.-F. Huang, C.-F. Li, G.-C. Guo, E.-M. Laine, H.-P. Breuer, and J. Piilo, Experimental control of the transition from markovian to non-markovian dynamics of open quantum systems, *Nature Physics* **7**, 931 (2011).
- [25] A. Smirne, D. Brivio, S. Cialdi, B. Vacchini, and M. G. Paris, Experimental investigation of initial system-environment correlations via trace-distance evolution, *Physical Review A* **84**, 032112 (2011).
- [26] S. Cialdi, A. Smirne, M. G. Paris, S. Olivares, and B. Vacchini, Two-step procedure to discriminate discordant from classical correlated or factorized states, *Physical Review A* **90**, 050301 (2014).
- [27] M. Gessner, M. Ramm, T. Pruttivarasin, A. Buchleitner, H.-P. Breuer, and H. Häffner, Local detection of quantum correlations with a single trapped ion, *Nature Physics* **10**, 105 (2014).
- [28] J.-S. Tang, C.-F. Li, Y.-L. Li, X.-B. Zou, G.-C. Guo, H.-P. Breuer, E.-M. Laine, and J. Piilo, Measuring non-markovianity of processes with controllable system-environment interaction, *Europhysics Letters* **97**, 10002 (2012).
- [29] G. A. White, C. D. Hill, F. A. Pollock, L. C. Hollenberg, and K. Modi, Demonstration of non-markovian process characterisation and control on a quantum processor, *Nature Communications* **11**, 6301 (2020).
- [30] G. Andersson, B. Suri, L. Guo, T. Aref, and P. Delsing, Non-exponential decay of a giant artificial atom, *Nature Physics* **15**, 1123 (2019).
- [31] R. Bulla, H.-J. Lee, N.-H. Tong, and M. Vojta, Numerical renormalization group for quantum impurities in a bosonic bath, *Physical Review B* **71**, 045122 (2005).
- [32] R. Bulla, T. A. Costi, and T. Pruschke, Numerical renormalization group method for quantum impurity systems, *Reviews of Modern Physics* **80**, 395 (2008).
- [33] R. P. Feynman and F. Vernon Jr, The theory of a general quantum system interacting with a linear dissipative system, *Annals of physics* **281**, 547 (2000).
- [34] M. Suzuki, *Quantum Monte Carlo methods in condensed matter physics* (World scientific, 1993).
- [35] R. Egger and C. Mak, Low-temperature dynamical simulation of spin-boson systems, *Physical Review B* **50**, 15210 (1994).
- [36] R. Egger, L. Mühlbacher, and C. Mak, Path-integral monte carlo simulations without the sign problem: Multilevel blocking approach for effective actions, *Physical Review E* **61**, 5961 (2000).
- [37] L. Mühlbacher, J. Ankerhold, and A. Komnik, Nonequilibrium dynamics of correlated electron transfer in molecular chains, *Physical review letters* **95**, 220404 (2005).
- [38] J. T. Stockburger and C. H. Mak, Stochastic liouvillian algorithm to simulate dissipative quantum dynamics with arbitrary precision, *The Journal of chemical physics* **110**, 4983 (1999).
- [39] J. T. Stockburger and H. Grabert, Exact c-number representation of non-markovian quantum dissipation, *Physical review letters* **88**, 170407 (2002).
- [40] Y. Tanimura and R. Kubo, Time evolution of a quantum system in contact with a nearly gaussian-markoffian noise bath, *Journal of the Physical Society of Japan* **58**, 101 (1989).
- [41] Y. Tanimura, Numerically “exact” approach to open quantum dynamics: The hierarchical equations of motion (heom), *The Journal of chemical physics* **153** (2020).
- [42] M. H. Beck, A. Jäckle, G. A. Worth, and H.-D. Meyer, The multiconfiguration time-dependent hartree (mctdh) method: a highly efficient algorithm for propagating wavepackets, *Physics reports* **324**, 1 (2000).
- [43] H. Wang and M. Thoss, Multilayer formulation of the multiconfiguration time-dependent hartree theory, *The Journal of chemical physics* **119**, 1289 (2003).
- [44] N. Makri and D. E. Makarov, Tensor propagator for iterative quantum time evolution of reduced density matrices. i. theory, *The Journal of chemical physics* **102**, 4600 (1995).
- [45] N. Makri, Quantum dissipative dynamics: A numerically exact methodology, *The Journal of Physical Chemistry A* **102**, 4414 (1998).
- [46] E. Gull, A. J. Millis, A. I. Lichtenstein, A. N. Rubtsov, M. Troyer, and P. Werner, Continuous-time monte carlo methods for quantum impurity models, *Reviews of Modern Physics* **83**, 349 (2011).
- [47] M. Xu, V. Vadimov, M. Krug, J. T. Stockburger, and J. Ankerhold, A universal framework for quantum dissipation: minimally extended state space and exact time-local dynamics (2023), arXiv:2307.16790 [quant-ph].
- [48] I. Vilkoviskiy and D. A. Abanin, A bound on approximating non-markovian dynamics by tensor networks in the time domain (2023), arXiv:2307.15592 [quant-ph].
- [49] K. Jacobs, *Quantum measurement theory and its applications* (Cambridge University Press, 2014).
- [50] L. D. Landau and E. M. Lifshitz, *Quantum mechanics: non-relativistic theory*, Vol. 3 (Elsevier, 2013).

- [51] A. Blais, A. L. Grimsmo, S. Girvin, and A. Wallraff, Circuit quantum electrodynamics, *Reviews of Modern Physics* **93**, 025005 (2021).
- [52] M. Collett and C. Gardiner, Squeezing of intracavity and traveling-wave light fields produced in parametric amplification, *Physical Review A* **30**, 1386 (1984).
- [53] C. W. Gardiner and M. J. Collett, Input and output in damped quantum systems: Quantum stochastic differential equations and the master equation, *Physical Review A* **31**, 3761 (1985).
- [54] B. Yurke and J. S. Denker, Quantum network theory, *Phys. Rev. A* **29**, 1419 (1984).
- [55] J. Combes, J. Kerckhoff, and M. Sarovar, The SLH framework for modeling quantum input-output networks, *Advances in Physics: X* **2**, 784 (2017).
- [56] M. Kjaergaard, M. E. Schwartz, J. Braumüller, P. Krantz, J. I.-J. Wang, S. Gustavsson, and W. D. Oliver, Superconducting qubits: Current state of play, *Annual Review of Condensed Matter Physics* **11**, 369–395 (2020), <https://doi.org/10.1146/annurev-conmatphys-031119-050605>.
- [57] F. Arute, K. Arya, R. Babbush, D. Bacon, J. C. Bardin, R. Barends, R. Biswas, S. Boixo, F. G. Brandao, D. A. Buell, *et al.*, Quantum supremacy using a programmable superconducting processor, *Nature* **574**, 505 (2019).
- [58] V. Vadimov, A. Viitanen, T. Mörstedt, T. Ala-Nissila, and M. Möttönen, Single-junction quantum-circuit refrigerator, *AIP Advances* **12** (2022).
- [59] M. Silveri, S. Masuda, V. Sevriuk, K. Y. Tan, M. Jenei, E. Hyyppä, F. Hassler, M. Partanen, J. Goetz, R. E. Lake, *et al.*, Broadband lamb shift in an engineered quantum system, *Nature Physics* **15**, 533 (2019).
- [60] J. Estève, M. Aprili, and J. Gabelli, Quantum dynamics of a microwave resonator strongly coupled to a tunnel junction (2018), arXiv:1807.02364 [cond-mat.mes-hall].
- [61] G. Aiello, M. Féchant, A. Morvan, J. Basset, M. Aprili, J. Gabelli, and J. Estève, Quantum bath engineering of a high impedance microwave mode through quasiparticle tunneling, *Nature Communications* **13**, 7146 (2022).
- [62] E. Hyyppä, S. Kundu, C. F. Chan, A. Gunyhó, J. Hotari, D. Janzso, K. Juliusson, O. Kiuru, J. Kotilahti, A. Landra, *et al.*, Unimon qubit, *Nature Communications* **13**, 6895 (2022).
- [63] L. Diósi, Non-markovian open quantum systems: Input-output fields, memory, and monitoring, *Phys. Rev. A* **85**, 034101 (2012).
- [64] J. Zhang, Y.-x. Liu, R.-B. Wu, K. Jacobs, and F. Nori, Non-markovian quantum input-output networks, *Phys. Rev. A* **87**, 032117 (2013).
- [65] J. A. Gross, B. Q. Baragiola, T. M. Stace, and J. Combes, Master equations and quantum trajectories for squeezed wave packets, *Phys. Rev. A* **105**, 023721 (2022).
- [66] V. Link, K. Müller, R. G. Lena, K. Luoma, F. Damanet, W. T. Strunz, and A. J. Daley, Non-markovian quantum dynamics in strongly coupled multimode cavities conditioned on continuous measurement, *PRX Quantum* **3**, 020348 (2022).
- [67] T. B. Propp, How to describe collective decay of uncoupled modes in the input–output formalism, *Journal of the Optical Society of America B* **39**, 3128 (2022).
- [68] W. D. Oliver and P. B. Welander, Materials in superconducting quantum bits, *MRS bulletin* **38**, 816 (2013).
- [69] J. M. Martinis, K. B. Cooper, R. McDermott, M. Steffen, M. Ansmann, K. Osborn, K. Cicak, S. Oh, D. P. Pappas, R. W. Simmonds, *et al.*, Decoherence in josephson qubits from dielectric loss, *Physical review letters* **95**, 210503 (2005).
- [70] R. Gordon, C. Murray, C. Kurter, M. Sandberg, S. Hall, K. Balakrishnan, R. Shelby, B. Wacaser, A. Stabile, J. Sleight, *et al.*, Environmental radiation impact on lifetimes and quasiparticle tunneling rates of fixed-frequency transmon qubits, *Applied Physics Letters* **120** (2022).
- [71] C. Wang, Y. Y. Gao, I. M. Pop, U. Vool, C. Axline, T. Brecht, R. W. Heeres, L. Frunzio, M. H. Devoret, G. Catelani, *et al.*, Measurement and control of quasiparticle dynamics in a superconducting qubit, *Nature communications* **5**, 5836 (2014).
- [72] R. Barends, J. Wenner, M. Lenander, Y. Chen, R. C. Bialczak, J. Kelly, E. Lucero, P. O’Malley, M. Mariantoni, D. Sank, *et al.*, Minimizing quasiparticle generation from stray infrared light in superconducting quantum circuits, *Applied Physics Letters* **99** (2011).
- [73] G. Catelani and J. P. Pekola, Using materials for quasiparticle engineering, *Materials for Quantum Technology* **2**, 013001 (2022).
- [74] D. Rainis and D. Loss, Majorana qubit decoherence by quasiparticle poisoning, *Physical Review B* **85**, 174533 (2012).
- [75] M. Xu, Y. Yan, Q. Shi, J. Ankerhold, and J. Stockburger, Taming quantum noise for efficient low temperature simulations of open quantum systems, *Physical Review Letters* **129**, 230601 (2022).
- [76] S. E. Nigg, H. Paik, B. Vlastakis, G. Kirchmair, S. Shankar, L. Frunzio, M. H. Devoret, R. J. Schoelkopf, and S. M. Girvin, Black-box superconducting circuit quantization, *Phys. Rev. Lett.* **108**, 240502 (2012).
- [77] F. Solgun, D. W. Abraham, and D. P. DiVincenzo, Black-box quantization of superconducting circuits using exact impedance synthesis, *Phys. Rev. B* **90**, 134504 (2014).
- [78] J. R. Schrieffer and P. A. Wolff, Relation between the anderson and kondo hamiltonians, *Physical Review* **149**, 491 (1966).
- [79] S. Bravyi, D. P. DiVincenzo, and D. Loss, Schrieffer–wolff transformation for quantum many-body systems, *Annals of physics* **326**, 2793 (2011).
- [80] A. O. Caldeira and A. J. Leggett, Path integral approach to quantum brownian motion, *Physica A: Statistical mechanics and its Applications* **121**, 587 (1983).
- [81] A. Schmid, On a quasiclassical langevin equation, *Journal of Low Temperature Physics* **49**, 609 (1982).
- [82] R. Benguria and M. Kac, Quantum langevin equation, *Physical review letters* **46**, 1 (1981).
- [83] G. Ford and M. Kac, On the quantum langevin equation, *Journal of statistical physics* **46**, 803 (1987).
- [84] G. W. Ford, J. T. Lewis, and R. O’Connell, Quantum langevin equation, *Physical Review A* **37**, 4419 (1988).
- [85] U. Vool and M. Devoret, Introduction to quantum electromagnetic circuits, *International Journal of Circuit Theory and Applications* **45**, 897 (2017).
- [86] Y. Nakatsukasa, O. Sète, and L. N. Trefethen, The aaa algorithm for rational approximation, *SIAM Journal on Scientific Computing* **40**, A1494 (2018).
- [87] J. Hubbard, Calculation of partition functions, *Physical Review Letters* **3**, 77 (1959).
- [88] R. Stratonovich, On a method of calculating quantum distribution functions, in *Soviet Physics Doklady*, Vol. 2 (1957) p. 416.

- [89] Q. Shi, Y. Xu, Y. Yan, and M. Xu, Efficient propagation of the hierarchical equations of motion using the matrix product state method, *The Journal of Chemical Physics* **148**, 174102 (2018).
- [90] R. Borrelli, Density matrix dynamics in twin-formulation: An efficient methodology based on tensor-train representation of reduced equations of motion, *The Journal of Chemical Physics* **150**, 234102 (2019).
- [91] J. Koch, T. M. Yu, J. Gambetta, A. A. Houck, D. I. Schuster, J. Majer, A. Blais, M. H. Devoret, S. M. Girvin, and R. J. Schoelkopf, Charge-insensitive qubit design derived from the cooper pair box, *Phys. Rev. A* **76**, 042319 (2007).
- [92] J. Gambetta, W. Braff, A. Wallraff, S. Girvin, and R. Schoelkopf, Protocols for optimal readout of qubits using a continuous quantum nondemolition measurement, *Physical Review A* **76**, 012325 (2007).
- [93] A. M. Gunyhó, S. Kundu, J. Ma, W. Liu, S. Niemelä, G. Catto, V. Vadimov, V. Vesterinen, P. Singh, Q. Chen, and M. Möttönen, Single-shot readout of a superconducting qubit using a thermal detector (2023), arXiv:2303.03668 [quant-ph].
- [94] D. Braun, F. Haake, and W. T. Strunz, Universality of decoherence, *Physical review letters* **86**, 2913 (2001).
- [95] J. Tuorila, J. Stockburger, T. Ala-Nissila, J. Ankerhold, and M. Möttönen, System-environment correlations in qubit initialization and control, *Phys. Rev. Res.* **1**, 013004 (2019).